New contributions to the ice-flow chronology in the Boothia–Lancaster ice-stream catchment area, Nunavut

T. Tremblay[1*] and M. Lamothe[2]

Abstract: Within the Boothia–Lancaster ice stream (BLIS) catchment area, ice-flow patterns were reconstructed based on the synthesis of striation directions and crosscutting relationships, transport patterns of erratic boulders, glacial landforms, cold-based glacial landsystems, and ice-retreat chronology. New ArcticDEM data, high-definition satellite imagery, and multibeam echosounder bathymetric data sets provided increased details on ice-flow indicators. Convergent high-velocity ice flows through the BLIS main axis were major, persistent features in the northeastern Laurentide Ice Sheet through the last glaciation, and this study highlights intensity fluctuations and ice-flow pattern variations that occurred during that time. Highly contrasting glacial geomorphology, notably in the abundance of moraines, reflects marked differences in ice-margin retreat rates and patterns during deglaciation between the western and eastern sides of the BLIS.

Résumé : Au sein du bassin d'alimentation du courant glaciaire de Boothia-Lancaster (CGBL), les configurations de l'écoulement glaciaire ont été reconstituées à partir de la synthèse des directions et des relations de recoupement des stries, des configurations de transport des blocs erratiques, des formes de terrain glaciaires, des systèmes de terrains glaciaires de glacier à base froide, et de la chronologie du retrait glaciaire. De nouvelles données d'ArcticDEM, des images satellite haute définition et des jeux de données de levés bathymétriques par échosondeur multifaisceaux fournissent de l'information détaillée sur les indicateurs de l'écoulement glaciaire. Des écoulements convergents à haute vitesse en direction de l'axe principal du CGBL furent majeurs et pérennes dans le secteur nord-est de l'Inlandsis laurentidien lors de la dernière glaciation, période durant laquelle la présente étude souligne les variations dans l'intensité et la configuration des écoulements glaciaires. Durant la déglaciation, la géomorphologie glaciaire contrastée entre les côtés ouest et est du CGBL, notamment dans l'abondance des moraines, témoigne de fortes différences dans la vitesse et la configuration du retrait glaciaire.

[1]Canada-Nunavut Geoscience Office, 1106 Inuksugait Plaza, P.O. Box 2319, Iqaluit, Nunavut X0A 0H0

[2]Département des sciences de la Terre et de l'atmosphère, Université du Québec à Montréal, 201, avenue du Président-Kennedy, Montréal, Quebec H2X 3Y7

*Corresponding author: T. Tremblay (email: tommy.tremblay@nrcan-rncan.gc.ca)

INTRODUCTION

The Boothia–Lancaster ice stream (BLIS) was a major glacial dynamic feature of the northeastern Laurentide Ice Sheet (NELIS) and the Innuitian Ice Sheet, forming a zone of fast ice flow channelled in the topographic depression that runs across Committee Bay, the Gulf of Boothia, Prince Regent Inlet, Lancaster Sound, and the northwestern part of Baffin Bay (Fig. 1). Many studies have contributed to the reconstruction of ice-flow patterns and chronology in the BLIS and surrounding areas (Prest et al., 1968; Dyke and Prest, 1987a; Andrews, 1989; Dyke and Dredge, 1989; Fulton, 1995; Dyke et al., 2002, 2003), including several that relied predominantly on satellite and digital elevation model (DEM)-based geomorphological interpretations (Boulton and Clark, 1990; Clark and Stokes, 2001; Kleman et al., 2006; De Angelis and Kleman, 2007; Margold et al., 2018). Outside of the study area, a relatively small fraction of the BLIS catchment area was part of the Innuitian Ice Sheet, mainly draining ice from Devon Island and the Wellington Channel (England et al., 2006). Although essential to glacial reconstructions of the NELIS, data on pre-deglacial phases of ice flow within the BLIS catchment area are generally scarce. Updating the current level of understanding of the history of the BLIS will require integrating historical and new geological and geomorphological observations on land and offshore with recent glaciological studies and numerical ice-sheet modelling results. This paper focuses on the last glacial maximum (LGM; Clark et al., 2009) and deglacial ice-flow patterns of the BLIS catchment area within the NELIS, using striation, glacial transport, and landform records. New ArcticDEM data, high-definition satellite imagery, multibeam bathymetric data sets, lithological composition of till, and stratigraphy documenting ice retreat are used to improve reconstructions of the local history of ice flow.

Previous work

The Quaternary geology of the study area (Fig. 1) was summarized at the regional or continental scale in several publications (Prest et al., 1968; Dyke and Prest, 1987a; Andrews, 1989; Dyke and Dredge, 1989; Fulton, 1995; Dyke et al., 2002, 2003). Sangamonian sediments are preserved on Boothia Peninsula and possibly on Prince of Wales Island, with no indication of deglaciation during the Wisconsinan prior to final deglaciation (Dyke and Matthews, 1987). On the coasts of northeastern Baffin and Bylot islands, the regional stratigraphy reflects several ice advances recorded by raised marine sediments dated using radiocarbon and amino-acid methods to the Middle Wisconsinan or earlier (Klassen, 1993). The Eclipse moraine on Bylot Island, thought to be associated with an ice stream in the Gulf of Boothia and Lancaster Sound (e.g. Dyke and Prest, 1987a), was then assigned a Middle Wisconsinan age, based on stratigraphic correlation with the pre-LGM marine sediments of northeastern Baffin and Bylot islands (Klassen, 1993). During the LGM, the presence of an ice shelf, rather than an ice stream, was suggested in the Gulf of Boothia and Lancaster Sound (Dyke and Prest, 1987b). Later, a Late Wisconsinan–Holocene age was reassigned to the Lancaster Sound–Boothia ice stream to reflect Late Wisconsinan (LGM?) ages assigned to the Eclipse and Navy Board moraines on Bylot and Baffin islands (Dyke and Hooper, 2001; Dyke et al., 2002, 2003).

The first reconstructions of LGM ice-flow patterns in the study area were proposed for Melville Peninsula (Sim, 1962), Baffin Island (Ives and Andrews, 1963), and Foxe Basin (Andrews and Miller, 1979). The LGM Laurentide Ice Sheet ice streams, broadly defined at the ice-sheet scale by Denton and Hughes (1981), were identified on Boothia Peninsula and Prince of Wales Island on the basis of detailed geomorphology and glacial transport patterns by Dyke (1984). Dyke and Morris (1988) later proposed some key considerations behind the ice-stream concept, including the convergence of streamlined landforms and the link between fine-grained tills and ice streams. Ice streams were subsequently identified from fieldwork on Melville Peninsula (Dredge, 1995), Bernier Bay (Hooper, 1996), Rae Isthmus (Dredge, 2002), and Steensby Inlet (Dyke, 2008). Deglacial geomorphology established patterns of ice retreat in northwestern Baffin Island (Dyke and Hooper, 2001). A large portion of the region was also covered by surficial geology mapping projects at the scale of 1:100 000 to 1:500 000 (*see* Kerr et al., this volume). Regional satellite and DEM-based geomorphological interpretations (Boulton and Clark, 1990; Clark and Stokes, 2001; Dyke and Hooper, 2001; Kleman et al., 2006; De Angelis and Kleman, 2007; Margold et al., 2018) reviewed the ice-flow chronology and the continuity of sets of converging, elongated glacial landforms over large areas indicative of ice streams, notably in the Gulf of Boothia and Lancaster Sound, during the LGM and deglaciation.

Figure 1. Location map, showing geographic regions and bedrock geology (*modified from* de Kemp et al., 2006 and Wheeler et al., 1996). Certain locations in the study area, outlined in white, are represented by letters: Kapuiviit (K), Milne Inlet (M), Moffet Inlet (Mo), Navy Board Inlet (N), Paquet Bay (P), Qiajivik Mountain (Q), and Whyte Inlet (W). The asterisk (*) indicates that Paleozoic carbonate rocks are inferred from bathymetric data interpretation. The locations of the seafloor macroform data sets are indicated by a black dot and corresponding number (*see* Fig. 3 for additional information on some of these locations). Location of the figures (Fig. 5–11) representing the seven geographic regions covered in this study is also shown.

75°N 95°W 85°W 75°W 75°N

Devon Island

Viscount Melville Sound

Resolute

Barrow Strait

Baffin Bay

Wellington Channel

Lancaster Sound

BLIS main axis

606
126
124

1067

Somerset Island

Northernmost Baffin Island

640

N

Bylot Island

324

Peel Sound

Prince of Wales Island

Prince Regent Inlet

Arctic Bay

Borden Peninsula

Admiralty Inlet

Tasiujaq

Pond Inlet

Pond Inlet

M'Clintock Channel

613

Bellot Strait

Figure 6

Boothia Peninsula and surrounding areas

Gulf of Boothia

Brodeur Peninsula

M

P

Q

612   114

Bernier Bay

Jungersen Bay

Northwestern Baffin Island

BAFFIN ISLAND

South of Pond Inlet

Barnes Ice Cap

70°N

Victoria Island

Larsen Sound

Boothia Peninsula

Saputing Lake

Gifford River

Figure 10

Steensby Inlet

70°N

Cape Victoria

Lord Mayor Bay

Taloyoak

Boothia Isthmus

107

Committee Bay

631

W

Fury and Hecla Strait

K

King William Island

Figure 5

94

Igloolik

Figure 9

Garry Bay

Gjoa Haven

101

Pelly Bay

Kugaaruk

Hall Beach

Melville Peninsula

Queen Maud Gulf

Rasmussen Basin

Adelaide Peninsula

Darby Lake

Figure 7 **Figure 8**

Barrow River

Chantrey Inlet

Northern Keewatin

Melville Peninsula

Foxe Basin

Garry Lake

Wager plateau

Rae Isthmus

Lyon Inlet

65°N

Kivalliq (Keewatin)

Naujaat

Aiviliup tariunga

65°N

Aberdeen Lake

Wager Bay

Baker Lake

Southampton Island

200 km

Coral Harbour

95°W   85°W

Elevation (m a.s.l.)

- 1500 – 3000
- 1000 – 1500
- 700 – 1000
- 600 – 700
- 500 – 600
- 400 – 500
- 300 – 400
- 200 – 300
- 0 – 200
- -100 – 0
- -300 – -100
- -800 – -300
- -5564 – -800

Bedrock geology

- Mesozoic-Cenozoic sedimentary rocks
- Paleozoic sedimentary rocks
- Paleozoic sedimentary rocks, inferred*
- Paleoproterozoic sediments
- Archean rocks
- ● Seafloor macroform data site

Study area context

The BLIS catchment area is bounded in the southwest by ice divides in Keewatin (Keewatin Ice Divide (KID), Lee et al., 1957; ancestral Keewatin Ice Divide (AK), Dyke and Prest, 1987a), which were connected to the Keewatin dome (KD) to the southwest, the M'Clintock Ice Divide (MID; Dyke, 1984b) in the west, and ice divides and saddles connected to the Foxe dome (FD) in the east (Dyke and Prest, 1987a). The FD and KD locations correspond to postglacial rebound maximums (Dyke and Prest, 1987a; Andrews and Peltier, 1989; Simon et al., 2016a). The complex ice-movement chronology related to the KID and AK migrations has been treated in several papers (Boulton and Clark, 1990; McMartin and Henderson, 2004; McMartin et al., 2021) and need not be dealt with here. Initially, also based on interpretations of the location of the postglacial rebound maximum (using the 10.5 ka cal. BP shoreline isobases), the location of the MID during the LGM was positioned over M'Clintock Channel (Dyke, 1984b), and later it was placed over eastern Victoria Island (Dyke and Prest, 1987b), western Prince of Wales Island (Dyke et al., 1992), Boothia Peninsula (De Angelis, 2007a), and Peel Sound (Stokes et al., 2016).

The area between Pelly Bay and western Committee Bay recorded some of the highest marine limits in the northern LIS, notably southeast of Boothia Peninsula (up to 240 m a.s.l.; Dyke, 1984b; Giangioppi et al., 2003; McMartin et al., 2015), where it is much higher than on the western side of Boothia Peninsula (Dyke et al., 2005). The differences in marine limit elevations on either side of this peninsula suggested a higher rate of ice retreat and an earlier deglaciation in the BLIS main axis in comparison to the region west of Boothia Peninsula (*see* Dyke et al., 2003).

Undated with absolute methods but attributed to the LGM on the basis of surface relationships with elongated streamlined landforms and a cover of only one sedimentary (marine) sequence, limits of the grounded ice associated with the BLIS in Baffin Bay are marked by faint grounding line features observed in multibeam bathymetric data at 1300 m depth (Brouard and Lajeunesse, 2017). The occurrence of recurring ice-rafted debris layers in Baffin Bay sediments might indicate important fluctuations in the output of glacial material from icebergs calving from ice shelves and fed by ice streams around northern Baffin Bay, including the ice shelf beyond Lancaster Sound linked with the BLIS (Andrews et al., 1998, 2014; Simon et al., 2012, 2014, 2016b).

Physiography and geology

The region largely comprises plateaus and some lowlands, dissected by deep, fault-bounded troughs, overdeepened by glacial erosion (Fig. 1). The plateaus range in height from 100 to over 600 m above sea level in the west and from 400 to over 800 m above sea level in the east; troughs typically reach a depth of between 100 and 300 m (800 m in Lancaster Sound). Glacier-covered mountains and high plateaus, up to 2000 m above sea level, are found on Bylot Island and eastern Baffin Island. The bedrock (Wheeler et al., 1996; de Kemp and Scott, 1998; de Kemp et al., 2006) consists dominantly of crystalline rocks (felsic gneiss, granite, and metamorphosed supracrustal rocks) from the Precambrian Canadian Shield; weakly metamorphosed Proterozoic sediments occur around Fury and Hecla Strait and on parts of Borden Peninsula and Bylot Island (de Kemp et al., 2006). Paleozoic carbonate rocks, with sandstone at the base in places, occur on parts of Boothia Peninsula, King William Island, western Baffin Island, and eastern Melville Peninsula, as well as on the seafloor of Foxe Basin, Lancaster Sound, the Gulf of Boothia, and Barrow Strait. Cretaceous to Paleogene sedimentary rocks, chiefly composed of poorly consolidated mudstone and sandstone, occur on Bylot Island, northern Boothia Peninsula, Somerset Island, and the seafloor of Lancaster Sound and Hudson Strait.

METHODOLOGY

This study integrates field observations and interpretations of ice-flow indicators and petrography of till clasts in the study area and refers to more than 30 publications relating to fieldwork conducted between 2000 and 2018. Remote-sensing-based mapping of geomorphological features at various scales, including glacial macroforms, the patterns of ice retreat and trajectories of subglacial meltwater drainage (eskers), and ice-front positions (ice-marginal moraines, ice-marginal channels), were also considered in the ice-flow reconstructions. Macroforms comprise streamlined landforms formed by subglacial activity (sliding), such as drumlins, megaflutings, megascale glacial lineations (MSGLs), crag-and-tail landforms, ice-moulded bedrock forms, and till plumes (carbonate and noncarbonate, as observed on satellite imagery; *see* Tremblay et al., 2016b; McMartin et al., 2021). The strong reliance on field data (including striations on bedrock) for synthesizing the paleoglacial flow patterns is similar to that of Veillette et al. (1999), for example. The ages presented in this study are in reservoir-effect-corrected calibrated years before present (cal. BP), and the ice-margin retreat boundaries are from Dalton et al. (2020), which presents a slightly modified version of Dyke et al. (2003) for most of the BLIS catchment area.

Superposition of geomorphological features commonly provided the relative chronology of events. The finest of two crosscutting sets (within striae or macroforms) was considered as being the youngest. For clarity, macroforms (and the interpreted flow sets) are presented as single arrows indicating the general direction of ice flow and relative chronology in a particular area (Fig. 2a, e). The directions of late deglacial ice-flow indicators were variable in some areas due to local relief and, for simplicity, those within 40° or less were represented by a single arrow. Within each deglacial phase (i.e. phase 3), ice-flow indicator arrows do not necessarily

Figure 2. Regional synthesis of complex ice-flow chronology from terrestrial field observations (mostly from striations, lithological contents of the till-pebble fraction, macroforms, and stratigraphic records) in the Boothia–Lancaster ice stream (BLIS) catchment area and from offshore data sets compiled from multiple studies. Dashed ice-flow directions represent directions of macroforms only (onshore and offshore). The phases are in general order of chronology relative to their time of initiation. The deglaciation ice-margin chronology mapped as thin black lines (with various line types) is in calibrated years, with ^{14}C years corrected for reservoir effect, taken from Dalton et al. (2020); this updated ice-margin chronology presents an almost unmodified version of Dyke et al. (2003) for most of the BLIS catchment area. **a)** Summary of regional ice-flow chronology indicators from multiple studies. (*See* legend in Fig. 2e.)
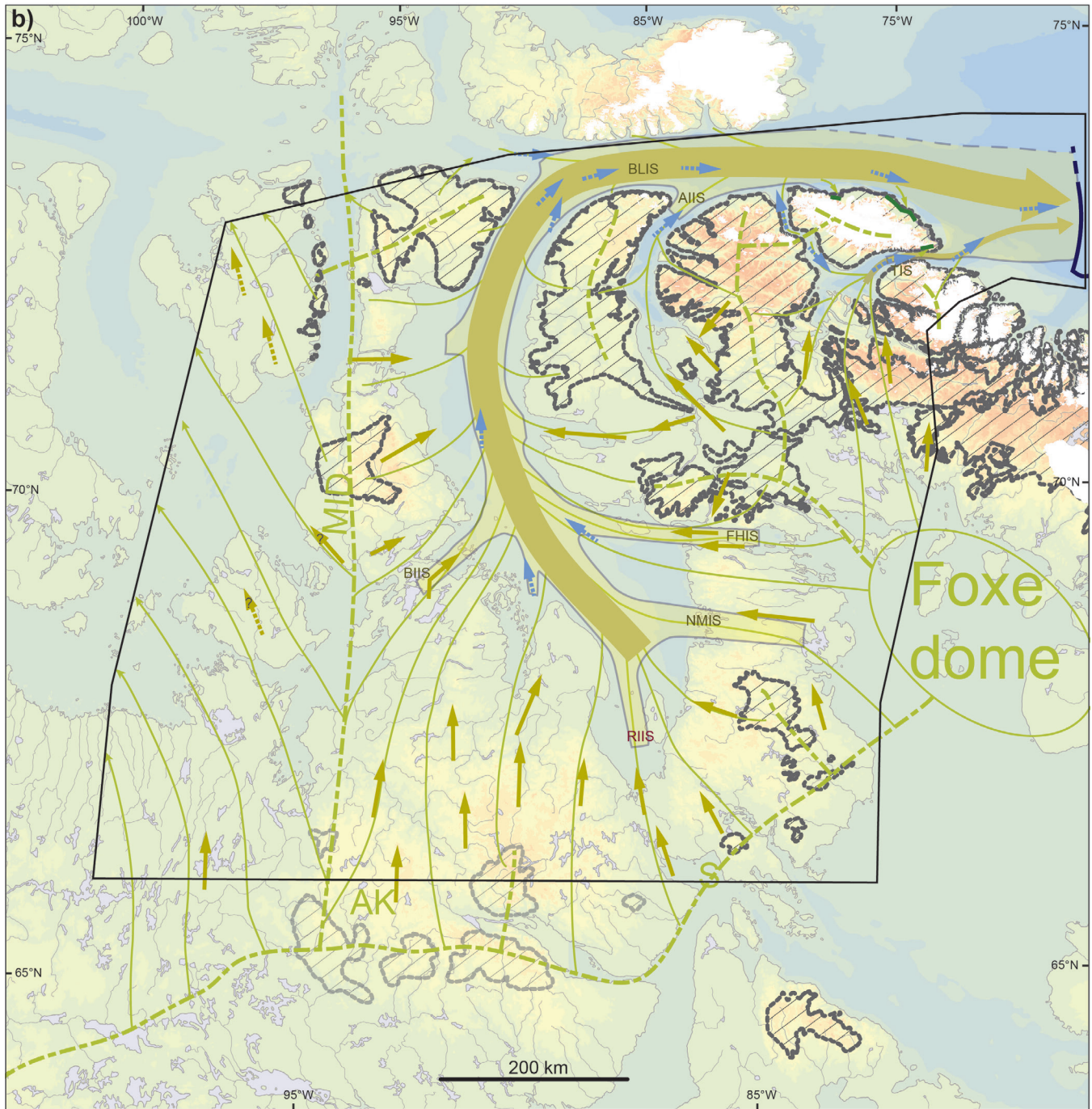
Figure 2. (cont.) b) Phase 1 ice-flow patterns, with position of the ancestral Keewatin Ice Divide (AK) and M'Clintock Ice Divide (MID). (*See* legend in Fig. 2e.)
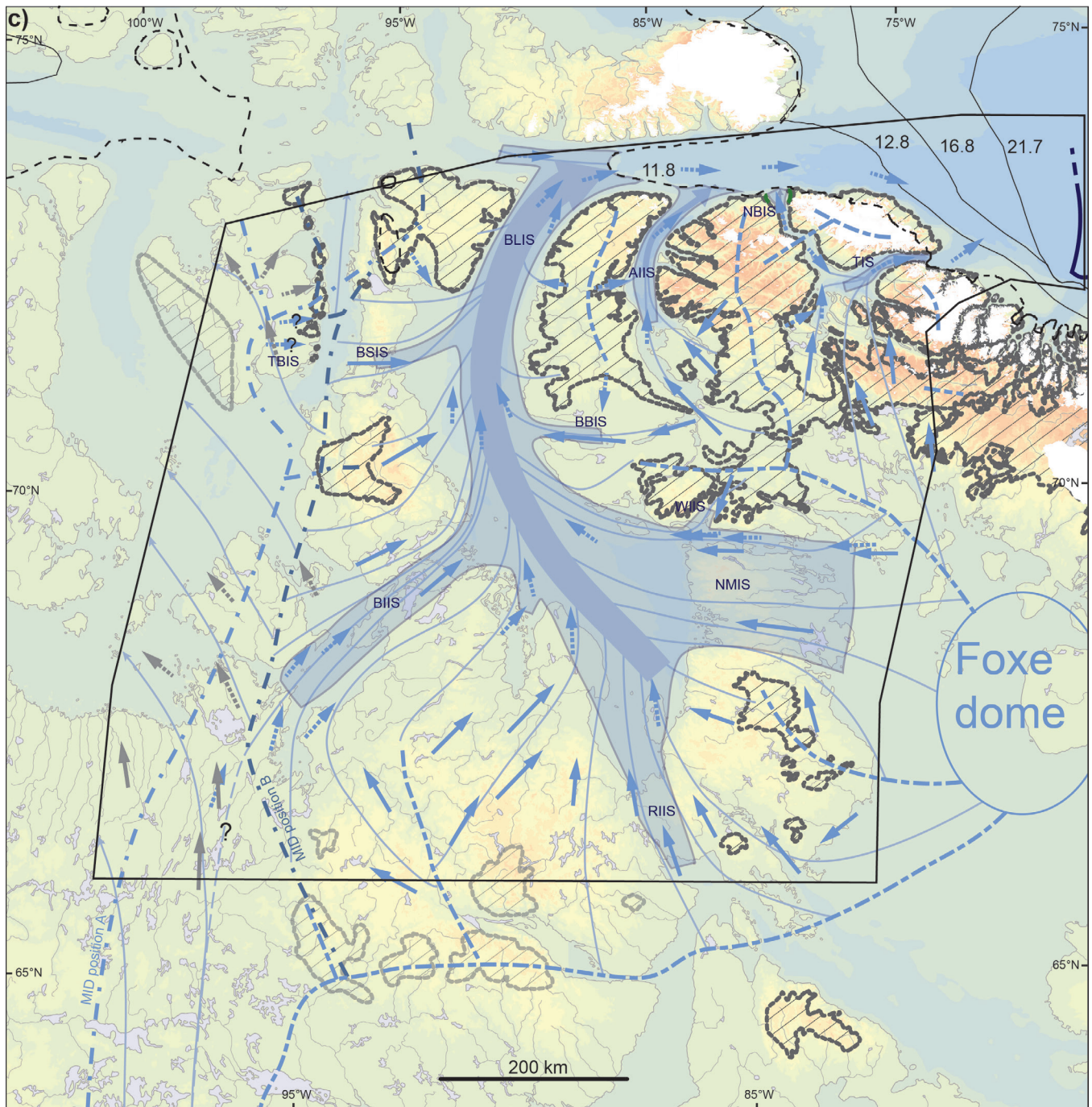
Figure 2. (cont.) c) Phase 2 ice-flow patterns. Phase 2 MID alternative configurations: 'A' represents the maximum BLIS ice catchment area comprising the area between Garry Lake and Adelaide Peninsula on the mainland, and eastern Prince of Wales Island; 'B' represents the minimum BLIS ice catchment area. (*See* legend in Fig. 2e.)
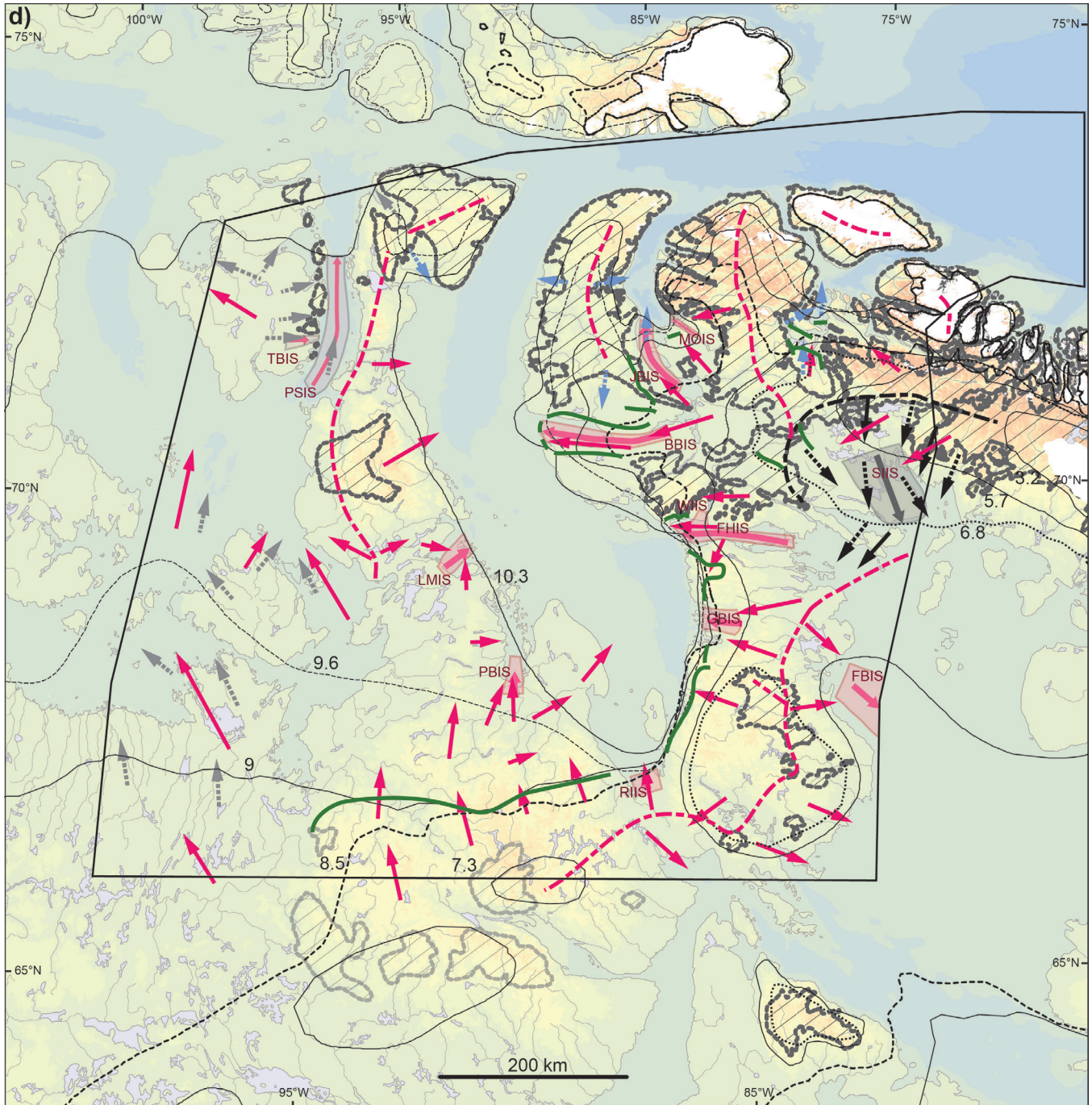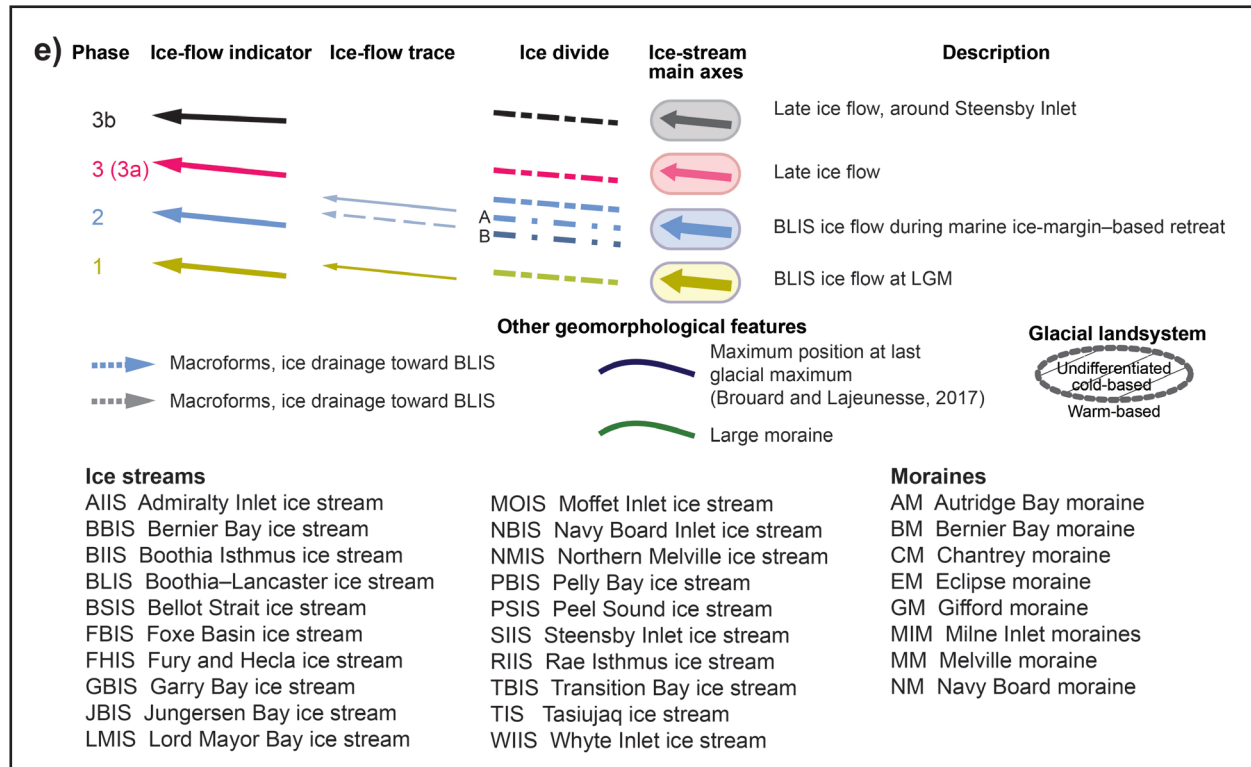
Figure 2. (cont.) d) Phases 3, 3a, and 3b ice-flow patterns. (*See* legend in Fig. 2e.)

Figure 2. (cont.) e) Common legend for Figure 2a–d. Note that not all the legend items may appear on each of these figures.

represent synchronous events. As the ice front was receding during deglaciation, ice flows varied in direction and were occurring in a time-transgressive manner.

RESULTS

Seafloor mapping

High-definition multibeam bathymetric data collected from the Canadian Coast Guard ship *Amundsen* during multiple expeditions (Ocean Mapping Group, 2019) were used to map submarine features, mainly megaflutings and drumlins, in the BLIS main axis, Fury and Hecla Strait, Foxe Basin, Admiralty and Navy Board inlets, as well as in the basins west of Boothia Peninsula. Local marine geology interpretations were incorporated from Lancaster Sound (Li et al., 2011; Bennett et al., 2014), the King William Island area (Shaw et al., 2019), and northwest of Baffin Island (Brouard and Lajeunesse, 2017, 2019). In places, landforms were not entirely mapped from the bathymetric data; however, images were generally clear enough to distinguish streamlined features from bedrock structures, other glacial landforms (eskers), or iceberg scour marks. The glacial macroforms on the seafloor indicated the last major ice-flow direction and that locally, the ice was in contact with the bed at the time, instead of floating. The locations of key, newly interpreted seafloor-macroform data sets are presented on

Figure 1, and Figure 2a–e shows the directions of ice-flow indicators and ice-flow traces inferred from them (and those from other studies). Images of seafloor topography in Navy Board Inlet (Fig. 3a), Peel Sound (Fig. 3b), and Lancaster Sound (Fig. 3c) represent examples of critical evidence for the geomorphological interpretation presented in the following sections.

Mapping of cold-based glacial landsystems

The mapping of various types of cold-based glacial landsystems (Dyke, 1993; Dyke and Evans, 2003; McMartin et al., 2021) allows identification of areas where, during most or part of the last glaciation, cold-based ice conditions existed. In the BLIS catchment area, cold-based glacial landsystems were delineated primarily from field observations (weathering of outcrops, presence of regolith, absence or scarcity of striations and roches moutonnées; Fig. 4a–e), aerial photographs, satellite imagery, and DEM interpretations (Tremblay and Paulen, 2012; Leblanc-Dumas et al., 2014; Tremblay et al., 2016a; Tremblay, 2017, 2018). Mapping undertaken in this study also incorporated results and concepts from previous geomorphological mapping in the northeastern Canadian Arctic (Dyke, 1993; De Angelis, 2007b), Baffin Island (Sugden and Watts, 1977; Sugden, 1978; Miller, 1980; Dyke et al., 1982; Andrews et al., 1985;
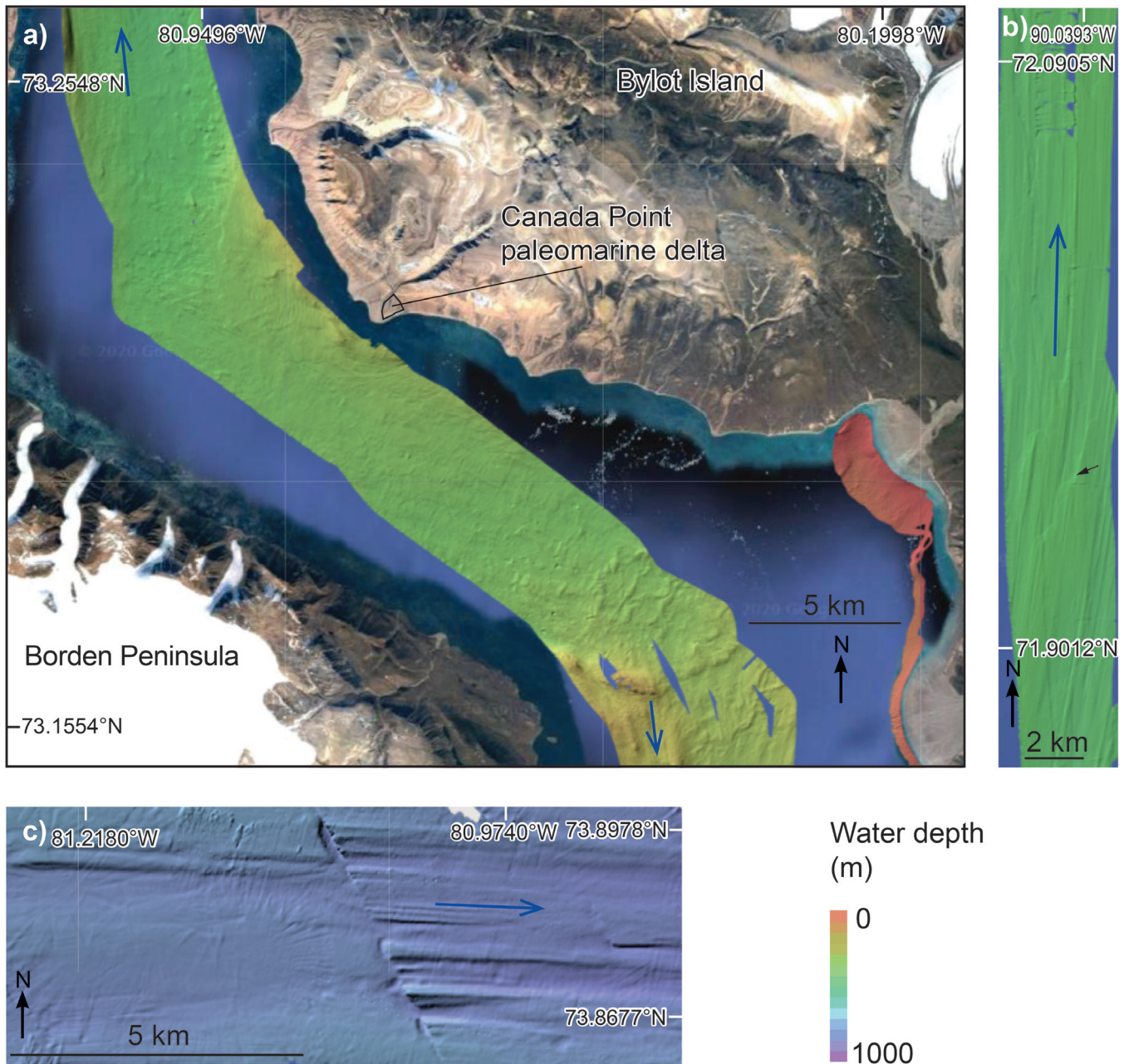
Figure 3. Seafloor features interpreted from multibeam bathymetric data (Ocean Mapping Group, 2019): **a)** central portion of Navy Board Inlet (site 324) showing an absence of streamlined landform indicative of cold-based conditions in the middle, also associated with the preserved pre-Wisconsinan Canada Point paleomarine delta (Klassen, 1993; Tremblay et al., 2020a), and streamlined landforms starting on either side of the cold-based zone (blue arrows); **b)** Peel Sound (site 613) with megaflutings (blue arrow) over flat seafloor probably underlain by Paleozoic carbonate rocks (with cuestas(?), shown by black arrow); and **c)** Lancaster Sound (site 1067) showing megaflutings and crag-and-tails (blue arrows). Location of the seafloor macroform sites can be found on Figure 1.
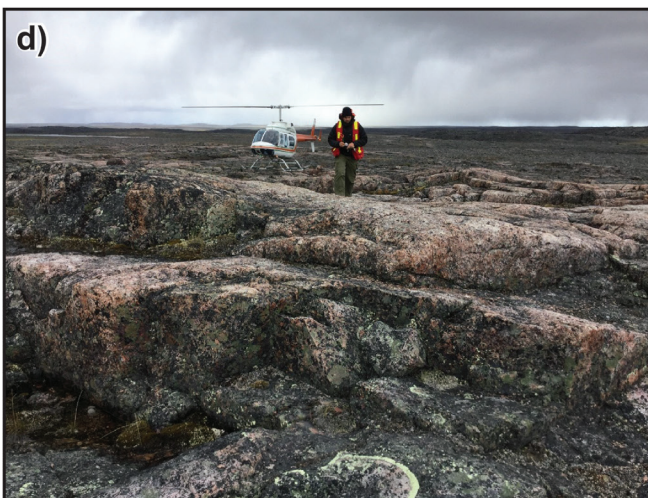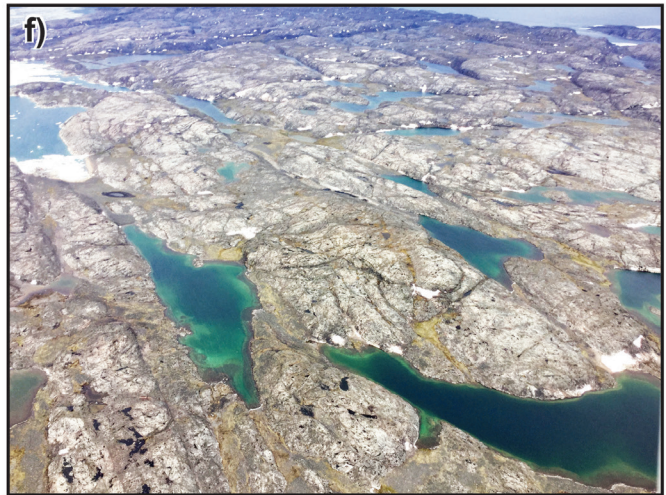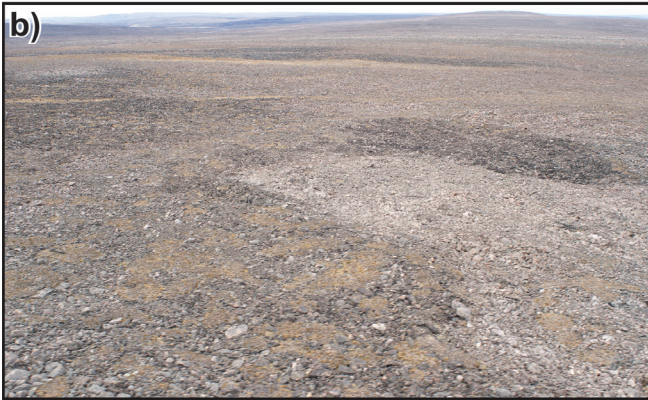
Figure 4. Field photographs typical of cold-based (CB), intermediate cold-based (IB), and warm-based (WB) glacial landscapes from north of Fury and Hecla Strait. **a)** Regolith and some regolith–till mix over Mesoproterozoic sedimentary rocks (CB); NRCan photo 2021-068. **b)** Regolith and regolith–till mix over Archean felsic and mafic intrusive rocks (CB); NRCan photo 2021-069. **c)** Regolithic bedrock exposed in glaciofluvial channel, with regolith and regolith–till mix in the background, over Archean felsic granitic gneiss (CB); NRCan photo 2021-070. **d)** Outcrop of Archean felsic granitic gneiss, with no preferential erosion features (such as roches moutonnées) or striations (IB); NRCan photo 2021-071. **e)** Roches moutonnées on gabbro dyke surrounded by till and regolith mix (warm-based to intermediate cold-based glacial landscape); NRCan photo 2021-072. **f)** Ice-moulded bedrock form in Archean granitic rocks (WB); NRCan photo 2021-073. **g)** Linear glacial erosion in Mesoproterozoic sedimentary rocks (WB); NRCan photo 2021-074. All photographs by T. Tremblay.

Marsella et al., 2000), Melville Peninsula (Dredge, 2000), and concurrent mapping in Keewatin by McMartin et al. (2021).

Most of the study area consists of warm-based glacial landscapes (*see* McMartin et al., 2021), displaying strong amounts of glacial erosion such as streamlined outcrops and bedrock hills (Fig. 4f), linear glacial erosion in fiords and glacial valleys (Fig. 4g), and various glacial macroforms. However, the cumulative amount of glacial erosion over the past glaciation(s) is spatially variable (Tremblay and Gosse, 2019) and, in some places, was not sufficiently intense to remove the inherited weathering of the bedrock and the regolith. The 'Undifferentiated cold-based' glacial landsystem identified in the legend (Fig. 2e) to Figure 2a–d refers to terrains that were subjected to varying duration and extent of cold-based conditions, as supported by geomorphological evidence of little to moderate amounts of glacial erosion and moderate to high proportions of weathered bedrock, and are, in many cases, a simplified version of the mapping presented in the field reports. For example, the regions mapped as undifferentiated cold-based glacial landsystems on the plateau north of Fury and Hecla Strait (Fig. 2a–e) refer to a mix of cold-based glacial landscapes (little to no evidence of glacial erosion; Fig. 4a, b, c) and intermediate cold-based glacial landscapes (little to moderate evidence of glacial erosion; Fig. 4d, e; *see* McMartin et al., 2021). In the core of a cold-based glacial landscape, there is a general absence of striations, roches moutonnées, and glacial macroforms; the ground is typically covered with a mix of regolith (Fig. 4a, b), boulders, weathered till, and glaciofluvial sediments often associated with ice-marginal channels (Fig. 4c). Crystalline bedrock is generally moderately to extensively weathered, occasionally dotted with tors (Dyke, 1993) and inselbergs interpreted to have been formed before the Quaternary glaciations (Tremblay, 2017). A small amount of glacial dispersal is sometimes observed, for example on central Baffin Island (Dredge, 2004; Bonham-Carter et al., 2019). Large mountainous regions of Baffin Island were designated as undifferentiated cold-based regions (Staiger, 2005). Nonetheless, locally there may be evidence of warm-based local glaciers in valleys and cirques. Also, in warm-based landscapes, some sectors may have experienced cold-based deglaciation, whereas in other areas the conditions were cold-based for most of the pre-deglacial ice-flow phases. Because of the iterative effects of glacial erosion, fluvial and glaciofluvial activity, and weathering on the landscape (Tremblay, 2018), in many places over the numerous plateaus of the study area, the boundaries between cold-based, intermediate cold-based, and warm-based zones are transitional, rarely appearing as sharp boundaries in the landscape.

Cold-based glacial landsystems were also detected using cosmogenic isotope data from northern Baffin Island (Staiger et al., 2006) and plateaus on Melville Peninsula and Boothia Peninsula (Tremblay and Gosse, 2019), as well as mineralogical data from Melville Peninsula and southern Baffin Island (Dredge, 2000; Leblanc-Dumas et al., 2015). In cold-based areas, the presence of minerals indicative of weathering (various clay minerals such as kaolinite) in surface diamictons and the higher concentrations of ^{10}Be indicating inheritance in surface diamictons and bedrock samples help to emphasize the distinction between more or less glacially eroded terrains (Staiger et al., 2006; Margreth et al., 2016).

Regional ice-flow synthesis

From the synthesis of general ice-flow indicator directions, glacial transport patterns, and cold-based glacial landsystem mapping (Fig. 2a), glacial flow events are parsed into three phases. Phases 1 and 2, the only phases for which flow lines (i.e. ice-flow traces) are presented (Fig. 2b, c), refer to the entire study area, whereas phase 3 is generally more local and occurred under a restricted ice cover during the late stages of deglaciation. For the purpose of this synthesis, the study area was divided into seven geographic regions sharing glacial history similarities (boundaries of these regions are shown on Fig. 1).

Lancaster Sound and Gulf of Boothia (BLIS main axis)

Phases 1 and 2

In the BLIS main axis, submarine macroforms, often MSGLs, are mapped in various locations from the seafloor topography data (Fig. 2a, 3a). Seabed morphology clearly indicates a spatial continuity of macroform directions from Prince Regent Inlet to Lancaster Sound; the continuity of macroforms is much less apparent from Barrow Strait to Lancaster Sound. Ice flow within or toward the main BLIS axis is also identified by occasional striations and terrestrial macroforms on the adjacent shores (Fig. 2a). Landforms perpendicular to ice flow on the seabed demarcate the LGM limit of the BLIS grounded ice in Baffin Bay (Brouard and Lajeunesse, 2017), about 100 km farther offshore than the limit shown in Dyke et al. (2003) and Dalton et al. (2020). On Bylot Island, Dyke and Hooper (2001) and Dyke et al. (2002) interpreted the Eclipse moraine as a frontal moraine, or lateral moraine, indicating diverging ice-flow patterns during the LGM at the limit of the ice stream located in Lancaster Sound (Dyke and Hooper, 2001; Dyke et al., 2002).

During phase 1, ice-streaming conditions existed in the deep marine trough between Committee Bay and Lancaster Sound, which acted as a channel for ice flowing out of the NELIS in a quasi-stable or growing mass-balance state, presumably during the LGM (Fig. 2b). Ice-streaming conditions continued during periods of rapid, marine-based ice-margin retreat within the BLIS main axis throughout phase 2 (Fig. 2c) and until the ice retreated to the coasts of Boothia Peninsula and Committee Bay at approximately 10.3 ka (phase 3; Fig. 2d). Figure 2c illustrates ice-flow directions during ice retreat of the BLIS marine ice front through Lancaster Sound at approximately 11.8 ka. The sea-bottom morphology suggests that the dominant source of ice flow within the Lancaster Sound part of the BLIS was transiting through the Gulf of Boothia, with a minor contribution from subsidiary ice flows in Barrow Strait and the Innuitian Ice Sheet.

Boothia Peninsula and surrounding areas

Phase 1

South of Boothia Isthmus, the oldest striations are directed to the north and found on surfaces protected from a main northeastern ice flow (Fig. 2b, 5; Ozyer and Hicock, 2006; Tremblay et al., 2007, 2009). Additionally, evidence for an early northward glacial transport of Paleo-proterozoic sedimentary clasts in till, prior to glacial transport and re-entrainment to the northeast during a later phase, is observed east of Rasmussen Basin (Tremblay et al., 2007). The striation record indicates that northward ice flow eventually merged with northeast (east) ice flow over Boothia Isthmus, where the early northward ice flow is no longer observed (Fig. 5; Tremblay et al., 2009; Tremblay, 2017). Phase 1 ice flow predates the main northeastern ice flow associated with an enhanced ice-stream activity over Boothia Isthmus at the beginning of ice retreat within the BLIS main axis (see phase 2 below).
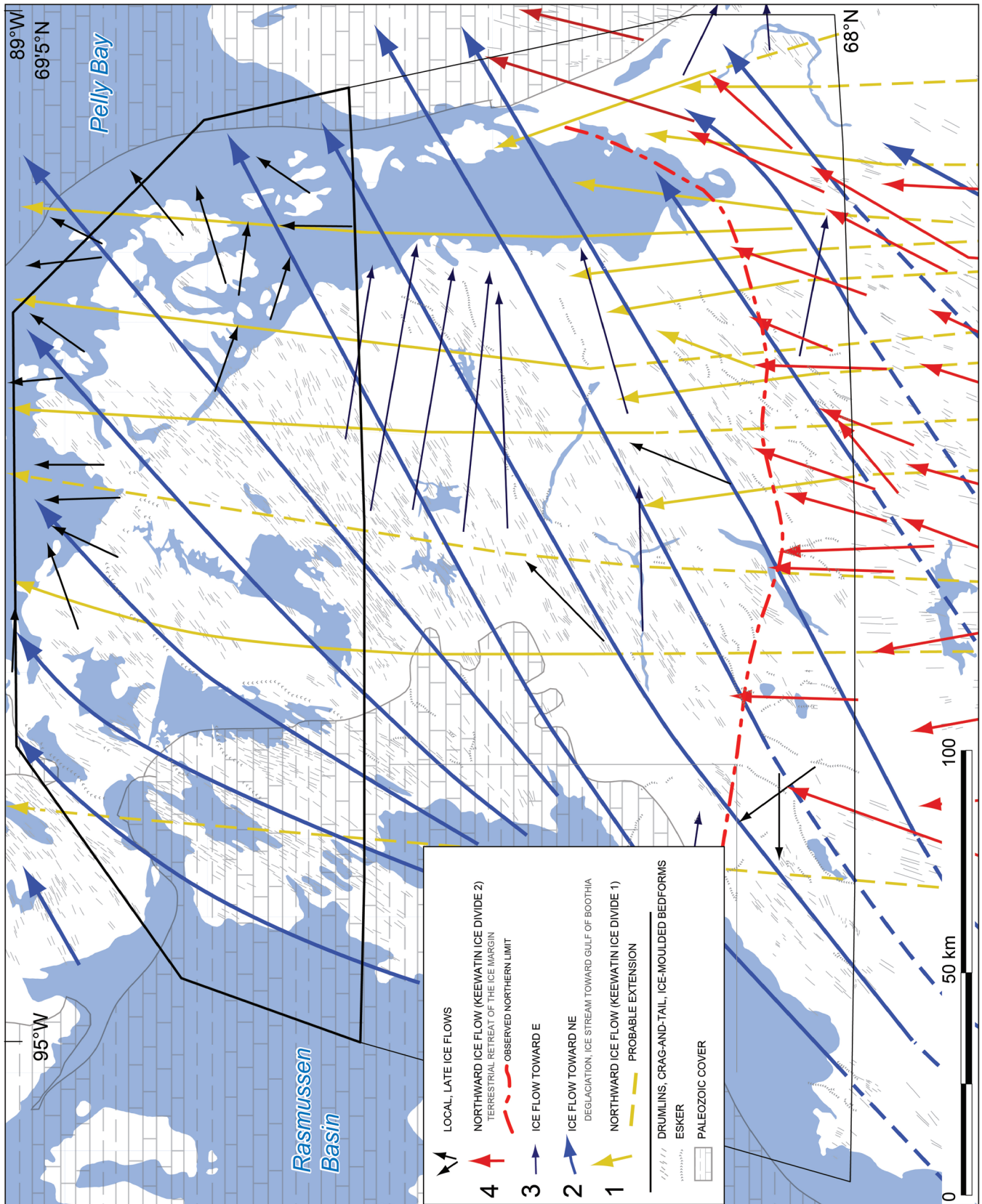
On Prince of Wales Island, an earlier north-northwest ice flow is indicated by the presence of Precambrian erratics over Paleozoic bedrock and north-northwest-aligned macroforms (Dyke et al., 1992). On King William Island, where no striations are reported on surficial maps (Helie, 1984), Ozyer (2011) suggested that similar northwest-aligned macroforms, also observed by Fulton (1995), might date from an early ice flow.

The early northward ice flow south of Boothia Isthmus, also observed in northern Keewatin (e.g. Ozyer and Hicock, 2006; McMartin et al., 2003), and the Boothia Isthmus subsidiary ice stream draining into the BLIS are attributed to ice-sheet buildup and the LGM. Although the timing of the early northward ice flow remains uncertain given the available data, it was probably active during the LGM because of the relatively high abundance of associated striations and the evidence of northward glacial transport. During this phase, the ice south of Boothia Isthmus was not directed toward the topographic lows in the Gulf of Boothia, but instead flowed northward in a normal direction from the KID, which observation supports the idea of relatively thick ice not significantly influenced by topography during that period (McMartin et al., 2003).

The mapping of cold-based terrains and the ice-flow patterns north of Boothia Isthmus and on Prince of Wales Island indicate that the MID central axis was probably anchored over central Boothia Peninsula and western Somerset Island, Peel Sound, and eastern Prince of Wales Island during phase 1, close to where Margold et al. (2018) placed the ice divide. During that time, the presence of active ice streams in Viscount Melville Sound and M'Clintock Channel (England et al., 2009) implies that the MID was located east of Prince of Wales Island (Stokes et al., 2009, 2012; Margold et al., 2018).

The attributed LGM age for phase 1 differs from that of Dyke et al. (1992), who assigned an Early Wisconsinan age for the north-northwest ice-flow pattern on Prince of Wales Island and a location for the MID over M'Clintock Channel at the LGM (Dyke and Prest, 1987b). Alternatively, the absence of absolute dating on the older striae south of

Figure 5. Ice-flow lines in northern Kivalliq, south of Boothia Isthmus (*from* Tremblay et al., 2009) and macroforms (*modified from* Dyke, 1984).

LEGEND

LOCAL, LATE ICE FLOWS

4 — NORTHWARD ICE FLOW (KEEWATIN ICE DIVIDE 2)
    — TERRESTRIAL RETREAT OF THE ICE MARGIN
    — OBSERVED NORTHERN LIMIT

3 — ICE FLOW TOWARD E

2 — ICE FLOW TOWARD NE
    DEGLACIATION, ICE STREAM TOWARD GULF OF BOOTHIA

1 — NORTHWARD ICE FLOW (KEEWATIN ICE DIVIDE 1)
    — PROBABLE EXTENSION

— DRUMLINS, CRAG-AND-TAIL, ICE-MOULDED BEDFORMS
····· ESKER
PALEOZOIC COVER

Pelly Bay

Rasmussen Basin

89°W
69°5'N
68°N
95°W

100   50 km   0

Boothia Isthmus could be indicative of an early northward ice flow formed during the Middle Wisconsinan, maybe during inception toward the LGM (*see* 'Discussion' section).

Phase 2

South of Boothia Isthmus, striations record ice flow to the northeast (Fig. 2c, 5, 6), crosscutting the previous northward flow (Tremblay et al., 2007, 2009). Paleoproterozoic erratics also indicate a strong northeast transport episode after the northward dispersion, forming a palimpsest glacial dispersal train (Tremblay et al., 2007). Based on striations and glacial transport patterns of kimberlite indicator minerals (KIMs) in glacial sediments south of Pelly Bay, Ozyer (2011) separated the northeast ice-flow indicators into three separate ice-flow events that are all attributed to phase 2 of this study, to which the northeast macroforms on northern Pelly Bay seafloor are also attributed.

On Boothia Isthmus, a major ice-flow event is associated with convergent ice flow toward the northeast and east, as indicated by striations, elongated macroforms (MSGLs) developed in fine-grained carbonate till, abundant glacially moulded bedrock forms, and long distances of glacial transport (Dyke, 1984b). A large dispersal train of carbonate till, approximately 200 km wide, indicates glacial transport of more than 100 km from source and is associated with the Boothia Isthmus ice stream (BIIS on Fig. 2c) (Dyke, 1984b; Tremblay et al., 2009). The Bellot Strait ice stream (BSIS on Fig. 2c) forms another important zone of convergent ice flow further north on the topographic saddle between northernmost Boothia Peninsula and adjacent Somerset Island. There, east-northeast ice-flow indicators are recorded by striations, macroforms, and the glacial transport of Paleozoic carbonate rocks over Precambrian basement (Dyke, 1984a, b).

Paleozoic carbonate erratics found in the cold-based zone of the Boothia Peninsula plateau (Tremblay, 2017) could have been transported for a short distance under cold-based northeastward ice flows across Boothia Peninsula during phase 2 (Fig. 6). This is similar to the short-distance transport of Paleozoic carbonate erratics across cold-based terrain in central Baffin Island (Dredge, 2004). On the central Somerset Island plateau, the presence of sparse but widespread Precambrian erratics over Paleozoic carbonate bedrock (Dyke, 1984a) suggests that the plateau was overridden by eastward or northeastward ice flows prior to or during the LGM (phase 1), or as part of this early deglacial phase (phase 2).

On southeastern King William Island, high-elongation ratio macroforms (MSGLs) in carbonate till oriented northeast are observed on land and from seafloor data (Shaw et al., 2019) and are associated with the strong ice-stream flow on Boothia Isthmus. Examination of the seafloor data suggests that the northeastward macroforms are continuous between southeastern King William Island and Boothia Isthmus.

On the eastern portion of Prince of Wales Island, several eastward converging ice-flow patterns are recognized (Fig. 2c). Among those, the Transition Bay ice stream (TBIS; Margold et al., 2015) comprises converging macroforms in carbonate till crosscutting earlier northwest macroforms. The converging macroforms are constricted between patches of cold-based landscapes over the hilly terrain along the coast characterized by a lack of macroforms, a scarcity of carbonate erratics (*see* Dyke et al., 1992) and carbonate plumes (satellite images), dendritic river systems, and a low lake density. The connection of these eastward ice-flow patterns with eastward striations and macroforms in the Bellot Strait area of northern Boothia Peninsula and southern Somerset Island appears to be interrupted by northward-aligned macroforms in Peel Sound (Fig. 2a). If connected, the glacial transport of carbonate erratics over the Bellot Strait area implies that the onset zone of the Bellot Strait ice stream must have reached Paleozoic carbonate outcrops between Peel Sound and Larsen Sound, possibly during phase 2 ice flow within a maximum BLIS catchment area (MID position A on Fig. 2c). Contrary to information presented on the geological map of Wheeler et al. (1996), bathymetric data indicate flat topography with subdued cuestas in Peel Sound (Fig. 3b), which suggests that sedimentary rocks may cover a large part of this marine through. Alternatively, basal entrainment from MID position B located in Peel Sound could also explain the glacial transport of carbonate till as part of the Bellot Strait ice-stream flow. Although the exact position of the MID remains unknown due to lack of field data (between hypothetical position A or B), the MID probably reached its most westward position on King William Island during this phase (Dyke, 1984b; Ozyer, 2011).

On Boothia Peninsula, northwest of Boothia Isthmus, northwest striations crosscut northeast striations (Tremblay, 2017). This late ice flow is associated with small northwest (west) macroforms on land (Dyke, 1984b; Tremblay, 2017) and on the adjacent seafloor (Shaw et al., 2019). The overprint of these late northwest-trending ice-flow indicators on northeast striations suggests the beginning of the eastward migration of the MID over northern Boothia Peninsula at the end of phase 2.

On Prince of Wales and King William islands, a complex system of north to northwest macroforms is recorded on land (Prest et al., 1968; Netterville et al., 1976; Dyke et al., 1992; De Angelis and Kleman, 2005; Margold et al., 2015) and on the seabed (Fig. 2a; Shaw et al., 2019). Several macroforms are directly linked with ice streams, or onset zones of ice streams, flowing toward the northwest (De Angelis and Kleman, 2005).

Phase 2 corresponds to ice flows connected with an ice stream in M'Clintock Channel (Clark and Stokes, 2001; De Angelis, 2007b).
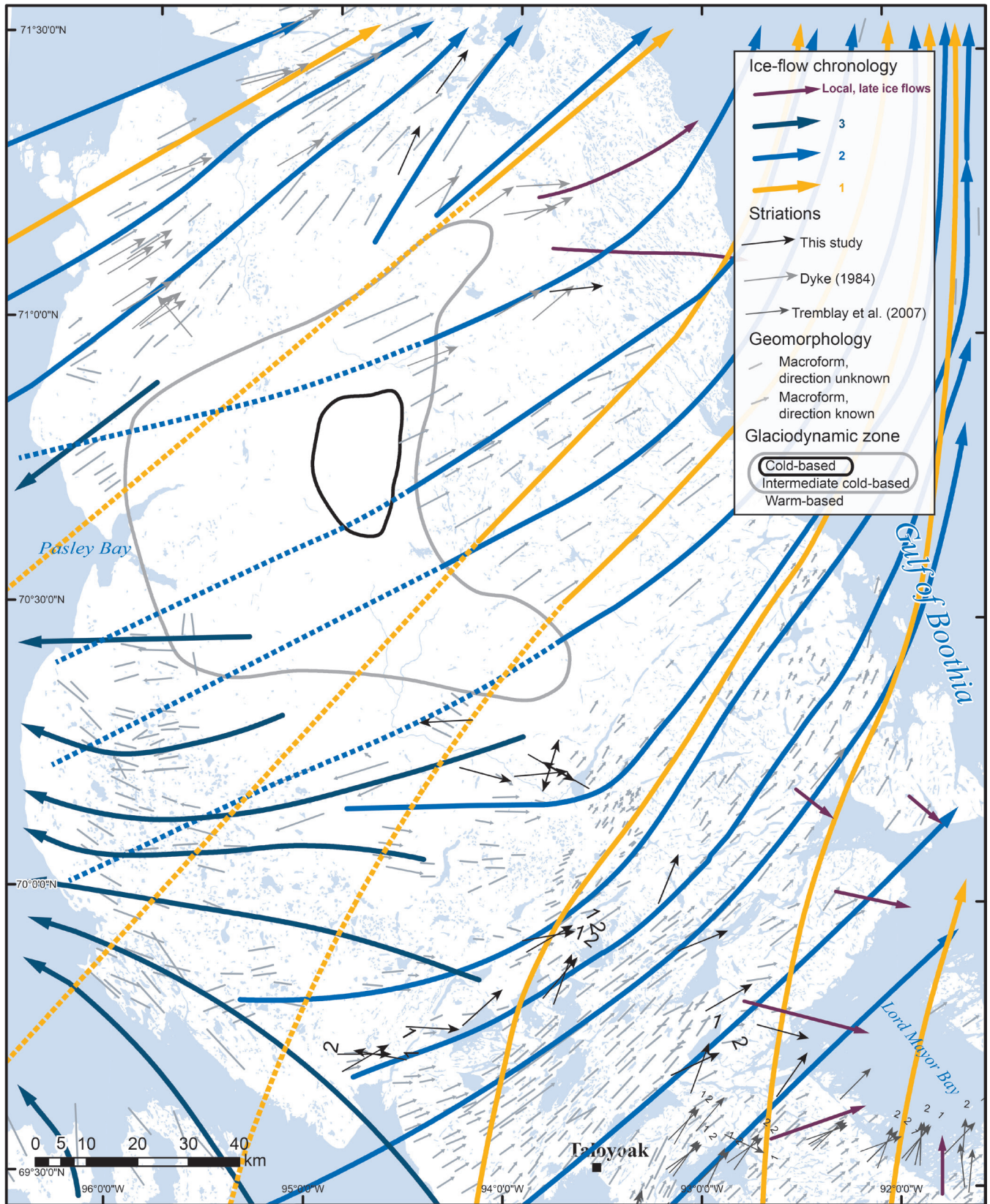
Figure 6. Striations (with age relationships), ice-flow lines, simplified geomorphological features (*modified from* Dyke,1984) and glaciodynamic zones south of Boothia Isthmus (*modified from* Tremblay, 2017). Dotted ice-flow line indicates weaker ice flow.

Phase 3

On the eastern coast of Boothia Peninsula, the latest striations indicate northeastward- and eastward-converging patterns toward Lord Mayor Bay (Tremblay et al., 2009; Tremblay, 2017) and Pelly Bay (Tremblay et al., 2007; Ozyer, 2011), which formed as a result of late, relatively small ice streams during phase 3 (Fig. 2d). The last remnant of the Boothia Isthmus ice stream was probably reduced to the smaller Lord Mayor Bay ice stream (LMIS on Fig. 2d), when the BLIS ice flow was waning following its former marine-based retreat to a terrestrial position. Local, late eastward ice flows toward Pelly Bay are also linked with minor re-entrainment of northeast dispersal trains of Paleozoic carbonate rocks and Paleoproterozoic marble (Tremblay et al., 2009). East of Darby Lake, late, fine northward striations crosscut northeast striations from phase 2 (Tremblay et al., 2007). South of Pelly Bay, a significant portion of the north to northeast glacial transport of KIMs (Ozyer, 2011) is thought to have occurred during phase 3.

Phase 3 occurred from 10.3 ka until deglaciation of the sector around 9 ka. Locally, phase 3 is characterized by sudden ice deflections, influenced by topography on land and coastal bathymetric slopes, normal to the shoreline. A complex network of short eskers and moraines, and the occurrence of ice-dammed glacial lakes on the plateaus, indicated a general southwestward ice retreat on southern Boothia Peninsula (Dyke, 1984b; Tremblay, 2017). At the latest stages of deglaciation, southwest- and southeast-retreating ice margins were moving toward an ice divide positioned in the middle of Boothia Peninsula and extending north of Somerset Island (Fig. 2d).

Northern Keewatin region

Phase 1

Over the Wager plateau, early northward striations are commonly found on protected lee surfaces of outcrops with prevalent northeastern striae (Little, 2001; McMartin et al., 2003, 2015; Ozyer and Hicock, 2006). This early northward ice flow was correlated with phase 1 south of Boothia Isthmus (see previous section), and an LGM age was attributed to it. An earlier southwest flow was recognized to the south of the study area (Taylor, 1956; Boulton and Clark, 1990; McMartin and Henderson, 2004; De Angelis and Kleman, 2005; McMartin and Dredge, 2005; Hodder et al., 2016) and attributed to the Early–Middle Wisconsinan, or a previous glaciation.

Phase 2

Between Wager plateau and Darby Lake, northeast striations and macroforms crosscut the earlier northward striae found on protected surfaces mentioned above and are attributed to phase 2. Between Chantrey Inlet and Darby Lake, northwest striations that also crosscut the earlier northward indicators (Little, 2001; Ozyer and Hicock, 2006) are therefore also assigned to phase 2 and are crosscut by later, northward striae associated with the Chantrey moraine system (see 'Phase 3' below). Ozyer (2011) suggested that the western extent of this northeastern ice flow (and therefore equivalent to the MID position at the time) was located beyond Adelaide Peninsula (hypothetical MID position A on Fig. 2c). Although northeastward-aligned macroforms are not present over the Adelaide Peninsula, the possibility that they have been eroded or obliterated by a later more northwesterly flow at the end of phase 2 implies that position A is still plausible. This is supported by the presence of north-northeast-trending MSGLs south of Adelaide Peninsula and superimposed northward macroforms curving to the northwest over the peninsula (McMartin et al., 2021).

During phase 2, as in the region south of Boothia Isthmus (see previous section), ice was drained toward the regional topographic lows (i.e. Committee Bay). Figure 2c shows a subsidiary ice divide separating the northeast ice flow toward the BLIS main axis from northwest ice flows feeding the Boothia Isthmus subsidiary ice stream. In contrast, McMartin and Henderson (2004) attributed this subsidiary ice divide to a later ice-flow phase, separating ice flow toward opening marine waters in Committee Bay from that in Chantrey Inlet, which would correspond to phase 3 of this study.

Phase 3

In northern Keewatin, phase 3 late deglacial ice flows commenced when the ice margin was near the coastline or in terrestrial positions (starting around 10.3 ka) and lasted until complete deglaciation of the KID sector around 7 ka (Fig. 2d). Northward ice flows are linked with the occurrence of a group of glaciomarine deltas near the marine limit north of Darby Lake (Tremblay et al., 2007) and to ice retreat to the Chantrey moraine system north of Wager plateau (Prest et al., 1968; McMartin and Henderson, 2004).
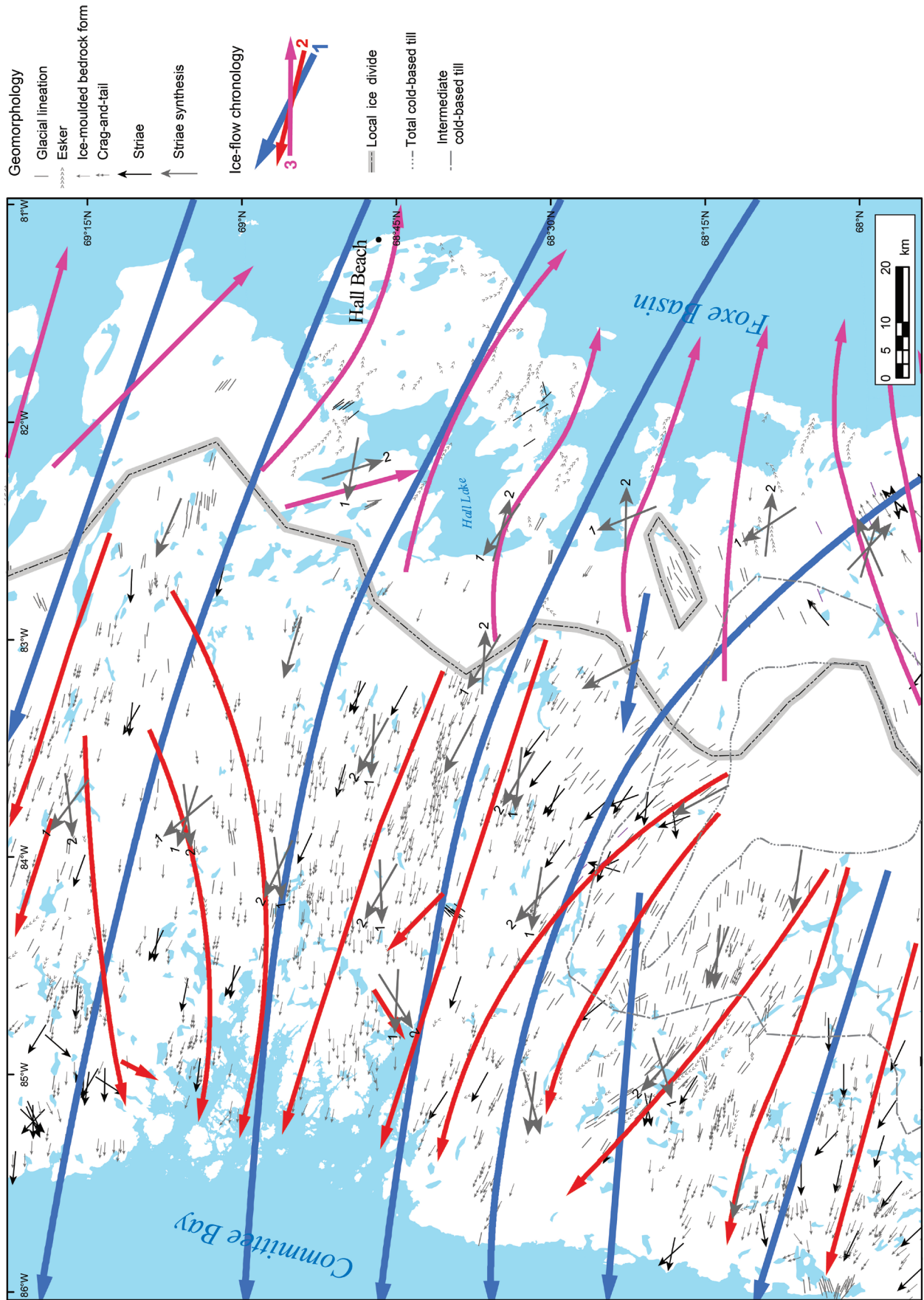
Melville Peninsula

Phases 1 and 2

In northern and western Melville Peninsula, west and northwest ice-flow directions converge toward the main axis of the BLIS as indicated by the directions of striations and macroforms (Fig. 7–9). Glacial transport of Paleozoic carbonate debris (Dredge, 2001, 2002) and clasts of Proterozoic marble and Archean supracrustal rocks (Tremblay and Paulen, 2012) is associated with this converging westerly ice flow (Fig. 8).
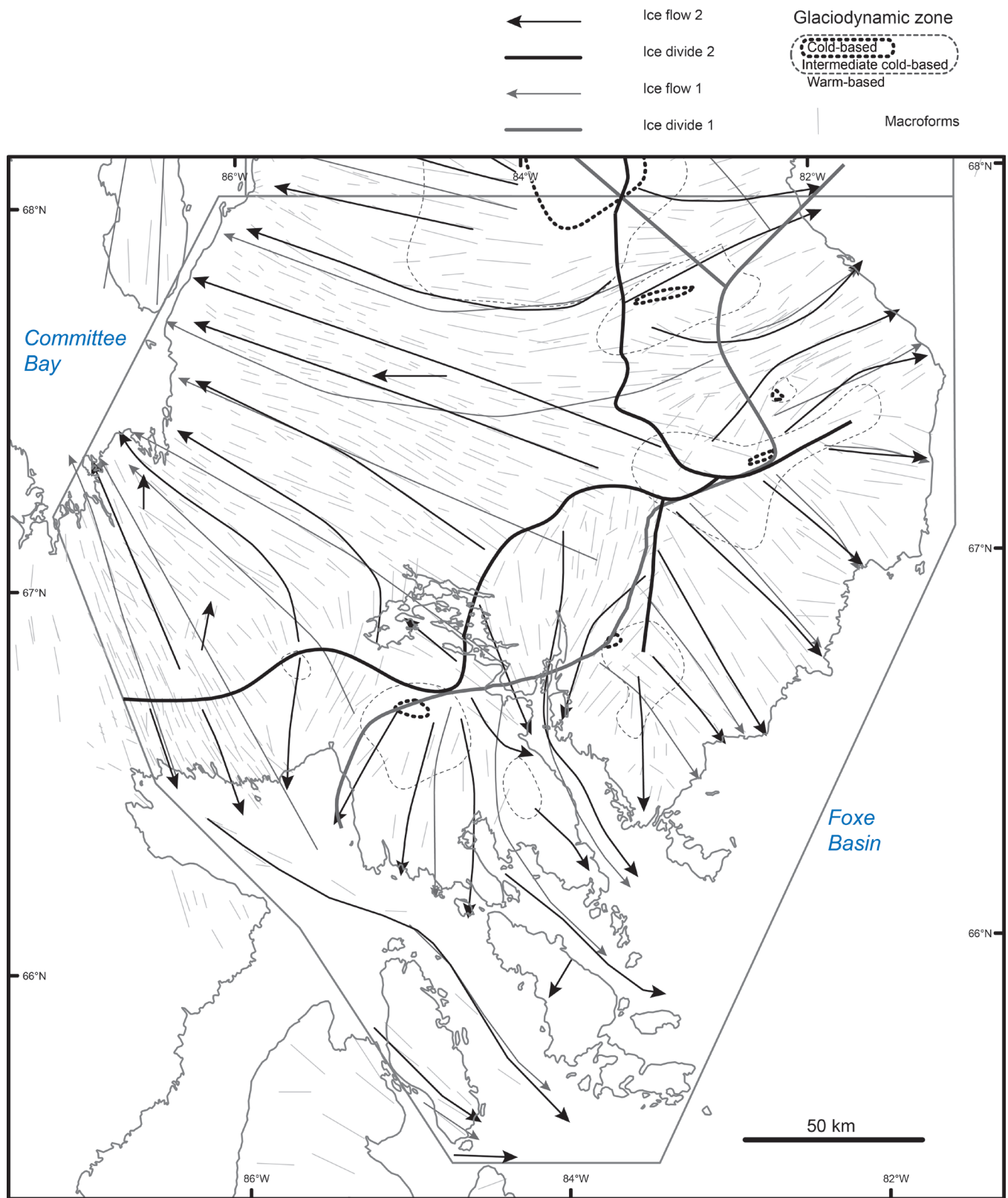
Figure 7. Ice-flow lines in the southern Melville Peninsula area (*from* Tremblay et al., 2016b) and glacial geomorphology (*modified from* Dredge, 1995, 2002).
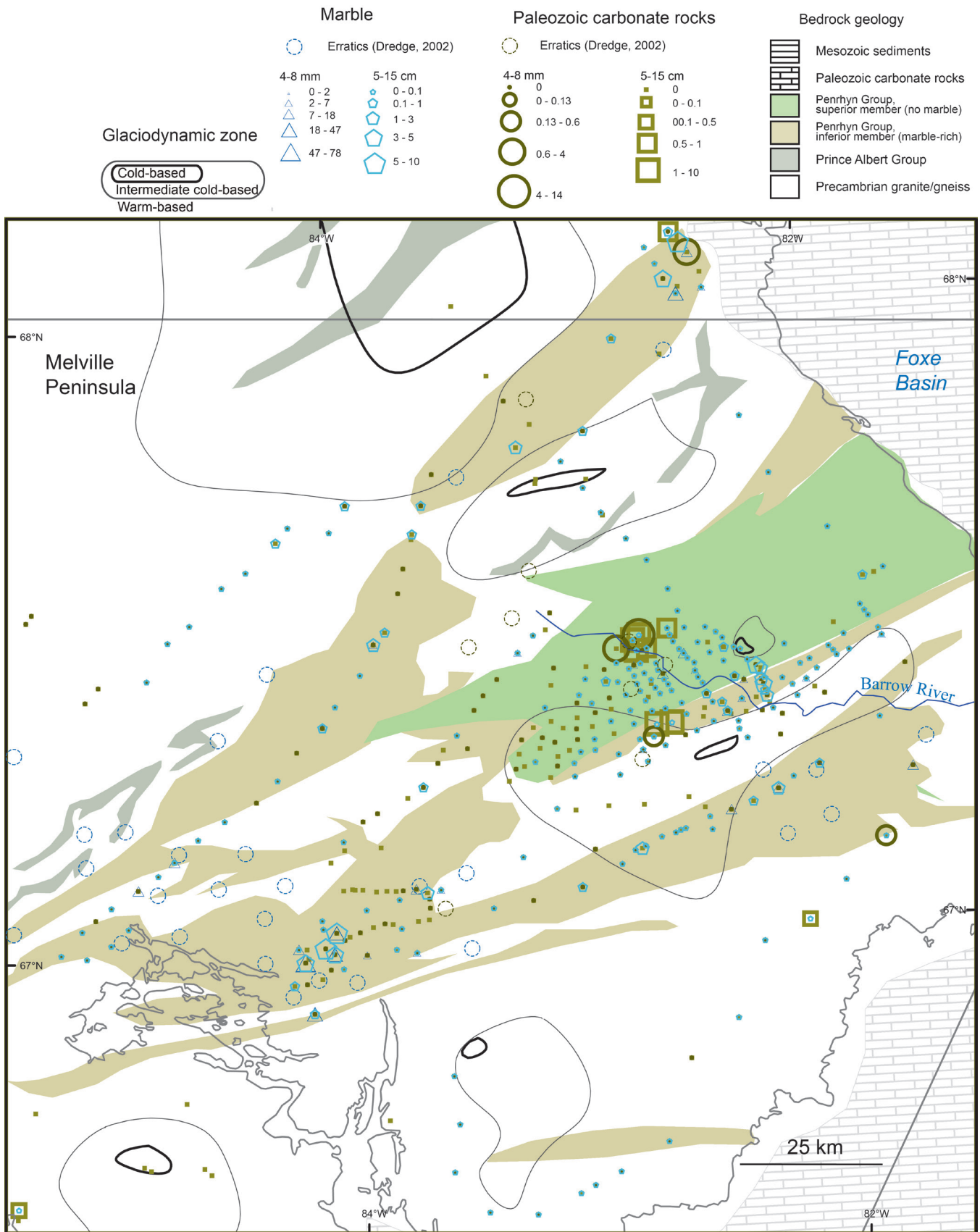
Figure 8. Petrographic counts in till pebbles (Tremblay et al., 2016b) and erratic boulder observations (Dredge, 2002), for Paleozoic carbonate rocks and Penrhyn Group marble (*from* Tremblay et al., 2016b).

Geomorphology

| Glacial lineation
∧∧ Esker
← Ice-moulded bedrock form
← Crag-and-tail
← Striae
← Striae synthesis

Ice-flow chronology

Local ice divide
Total cold-based till
Intermediate cold-based till

Figure 9. Ice-flow lines in the northern Melville Peninsula area (*from* Tremblay and Paulen, 2012), with glacial geomorphology (including new satellite-image interpretation) and associated elements (Dredge 1995, 2002; De Angelis, 2007a).

In the southeastern part of Melville Peninsula, evidence of ice crossing over the interior plateau from Foxe Basin is ambiguous. Only rare, early striations toward the northwest and west are present near the coast (Dredge, 2001). Cold-based terrains cover a portion of the southern Melville Peninsula plateau (Fig. 7), so Dredge (2001) presumed that any ice crossing over southern Melville Peninsula plateau would have been largely cold-based. A few, even earlier, southwest striae and drumlins occur in the same area, but these are associated with a radial flow pattern around Melville Peninsula during the Early Wisconsinan ice build-up phase (Dredge, 2002). Dredge (2001) suggested that an early, subsidiary ice divide from the FD (Melville ice divide) ran across the southern part of the peninsula during the LGM and early deglaciation (i.e. phase 1 and 2 in this study), and possibly during earlier Wisconsinan glaciations.

On the other hand, Paleozoic carbonate boulders are found over Precambrian bedrock of the southern Melville Peninsula plateau (Dredge, 2002; Tremblay et al., 2016b), indicating that some westerly glacial transport from Foxe Basin occurred across this plateau. Because of the absence of any fine-grained carbonate matrix associated with these boulders, Dredge (2001) suggested that the few lone Paleozoic carbonate boulders might have been deposited during pre-Sangamonian glaciations and that the calcareous matrix component had since weathered away. However, around Barrow River, glacial sediments contain Paleozoic carbonate pebbles and calcareous fine-grained material in two zones (Tremblay et al., 2016b). Paleozoic carbonate clasts also occur in till, forming a narrow band along the southeastern coast of Melville Peninsula (Dredge, 2002; Tremblay et al., 2016b). On this basis, Tremblay et al. (2016a) proposed that Paleozoic carbonate tills observed in valleys around Barrow River were deposited from a nearby unmapped Paleozoic carbonate outlier, therefore not invoking ice flow out of Foxe Basin. Alternatively, the Barrow River carbonate tills could also represent remnants of a former carbonate-till plume that crossed southern Melville Peninsula from Foxe Basin. Although the exact timing of this carbonate dispersal remains uncertain, it would represent the only area of southern Melville Peninsula with evidence of glacial transport from Foxe Basin during the Wisconsinan glaciations.

In summary, neither Dredge (2001) nor Tremblay et al. (2016a) presented unequivocal evidence of ice flow crossing from Foxe Basin over the southern Melville Peninsula plateau during phase 1 and phase 2. This would suggest that a portion of the ice divide (saddle) between the KD and FD (Dyke and Prest, 1987b) could have been located over southern Melville Peninsula during phase 1 and that it migrated to the southeast of Melville Peninsula during phase 2. On the

basis of assumptions relative to the increasing intensity of the BLIS during phase 2, a minimum BLIS catchment area is sketched for phase 1, and a maximum BLIS catchment area is drawn for phase 2 (Fig. 2b, c).

Phase 3

On the Committee Bay coast of Melville Peninsula, late ice flows with orientations varying between north-northwest and south-southwest are contemporaneous with the establishment of the Melville moraine (Dredge, 1995). On the western Melville Peninsula plateau, ice-flow directions during this later phase are only slightly different from those of phase 2 but suggest an increasing influence by local topography. A convergent ice-flow pattern, indicative of a waning northern Melville ice stream, is observed in Garry Bay (Garry Bay ice stream). On the northernmost tip of Melville Peninsula, late south and southwestward striations and southwest-oriented glacial transport of Mesoproterozoic quartz arenite are observed, heading toward an east–west-oriented section of the Melville moraine (Dredge, 2001).

Ice flows during phase 3 started around 10.3 ka, when the ice margin in contact with marine waters retreated near the coastline, and continued to be active along a stillstand position during the deposition of the Melville moraine, from 9.6 ka until about 7.5 ka (Dredge, 2001).

On Melville Peninsula, easterly indicators crosscut westerly ice-flow indicators locally, reflecting a northwestern migration of the ice divide to the centre of the peninsula (Fig. 2d) from a position in Foxe Basin during the previous phase 2. On the eastern coast of Melville Peninsula, ice flow toward the southeast, east, and northeast is indicated by striations, glacial transport of Precambrian crystalline rocks and chromite grains over Paleozoic bedrock, and macroforms (Fig. 7, 9; Tremblay and Paulen, 2012). Significantly, several southeast ice-flow striations crosscut the earlier west-north-west ice-flow indicators (phase 2; Fig. 2a). Across central Melville Peninsula (North Arrow Minerals Inc., 2018) and Rae Isthmus (Kupsch and Armstrong, 2013), KIM dispersal trains indicate late glacial transport toward Foxe Basin. Late ice flows in south-central Melville Peninsula are indicated by complex striations (west, south, east, northeast) toward Aiviliup tariunga (formerly Repulse Bay) and Foxe Basin that crosscut northwest to north-northwest ice-flow indicators converging into Committee Bay. A major, converging ice-flow reversal during late deglaciation toward Aiviliup tariunga and Roes Welcome Sound in adjacent Keewatin documented by McMartin et al. (2015) can be associated with the latest part of phase 3, when marine waters began

to open in northern Hudson Bay. Late southeast, east, and northeast ice flows toward ice streams draining Foxe Basin via Hudson Strait were major features on the eastern coast of Melville Peninsula. The ice divide separating easterly ice flows from northwesterly ice flows continued to migrate northwestward to its final position shown on Figure 2d.

On southeastern Melville Peninsula, the latest part of phase 3 would have started when the ice flows toward BLIS were waning (before or at 10.3 ka) and the Hudson Strait catchment area began to capture some of the ice flows from the BLIS catchment area. Phase 3 lasted until ice retreated near the coastline slightly before 7.3 ka. Terrestrial ice retreat toward small residual ice caps occurred between 7.3 ka and about 6 ka (Dredge, 2001).

Northwestern Baffin Island

Phases 1 and 2

The glacial geology of northwestern Baffin Island is characterized by the presence of several converging features indicated by macroforms and striations and forming ice-stream landsystems (Fig. 1, 2a-e, 10, 11): Bernier Bay, converging toward the Gulf of Boothia (Hooper, 1996); Fury and Hecla Strait, converging toward Committee Bay (Tremblay and Godbout, 2018); Whyte Inlet, converging toward Fury and Hecla Strait (Tremblay and Godbout, 2018); Admiralty Inlet, converging toward Lancaster Sound; and Moffet Inlet. Abundant elongated streamlined glacial landforms are present on the seafloor of the Fury and Hecla Strait (Tremblay and Godbout, 2018) and west of Bernier Bay (Fig. 11; Tremblay, 2021). Numerous ice-moulded-bedrock hills indicating a converging westerly flow were recorded on the shores of Fury and Hecla Strait (Fig. 10). Important glacial transport distances (up to 100 km) were reported within the Bernier Bay ice stream (Hooper, 1996), Admiralty Inlet ice stream (Dyke and Hooper, 2000; Tremblay, 2021), and Fury and Hecla ice stream (Hooper, 1996; Tremblay and Godbout, 2018; Tremblay et al., 2020b).

The ice streams are separated by plateaus, over which cold-based conditions persisted during at least phases 1 and 2. The Saputing Lake–Gifford River plateau, mostly covered by cold-based terrains, separates the northern Melville Peninsula area from the rest of Baffin Island. It is strategically located to allow the detection of glacial transport from a radial flow out of northern Melville Peninsula versus a flow into the BLIS because cold-based zones can preserve glacial erratics for a long period of time due to slow erosion rates. Figure 10

(*from* Tremblay and Godbout, 2018) shows the absence of Paleozoic carbonate rocks and Mesoproterozoic sedimentary rocks (chiefly indurated quartz arenite) in the clast fraction of glacial sediments over the Saputing Lake–Gifford River plateau and their abundance south of the plateau. This supports the idea that the ice did not flow northward to cross the cold-based Saputing Lake–Gifford River plateau and that the BLIS was active during the LGM and possibly during previous Wisconsinan glaciations (Dyke and Prest, 1987b; De Angelis, 2007a; Margold et al., 2018), in contrast with earlier reconstructions (Denton and Hughes, 1981; Mayewski et al., 1981). East of southern Admiralty Inlet, no Precambrian erratics were found over the core of the Paleozoic carbonate plateau (Tremblay, 2021), suggesting ice did not flow northeastward across Borden Peninsula.

Phase 1 occurred during late ice buildup to the LGM (Fig. 2b) and phase 2, from the LGM to around 13 ka, when the BLIS was at its most active phase of retreat (Fig. 2c), ending around 10.3 ka, when marine ice margins retreated near the coastline (Fig. 2d).

Phase 3

When the ice front was near the coastline, the Bernier Bay ice stream, Admiralty Inlet ice stream, Moffet Inlet ice stream, and Fury and Hecla Strait ice stream (BBIS, AIIS, MIIS, FHIS on Fig. 2d) were still active and formed numerous frontal and lateral moraines. The Bernier Bay moraine was deposited by lateral divergent ice flows, from the down-ice segment of warm-based ice within the Bernier Bay ice stream. Similarly, the Autridge Bay moraine (Fig. 10) and the associated northernmost, northwest-trending portion of the Melville moraine were deposited by down-ice divergent warm-based flow within the Fury and Hecla Strait ice-stream system (Fig. 2a). The Whyte Inlet ice stream (WIIS on Fig. 2d) was active as a tributary to the Fury and Hecla Strait ice stream, until the ice retreated around 9 ka.

On the Saputing Lake–Gifford River plateau, as ice receded over the land gradually from 10.3 to 6.8 ka, the orientation of the ice margin was often different from directions suggested during phase 2, as indicated by eskers, moraines, marginal channels, and proglacial lake configurations (Dyke and Hooper, 2001; Dyke, 2008; Tremblay and Godbout, 2018). The frequent absence of striations and macroforms associated with the pattern of ice retreat was probably associated with sluggish, cold-based ice flow, in some places accounting for the deposition of cold-based moraines (e.g. Gifford moraine).

Figure 10. Glacial events north of Fury and Hecla Strait, from striations, glacial macroforms, and petrographic counts in till (*from* Tremblay and Godbout, 2018). Digital elevation model (Porter et al., 2018) also shows the surficial geology (Hooper, 1996; Dyke and Hooper, 2001) and bedrock geology (de Kemp and Scott, 1998).

Bedrock geology map and petrographic counts in till (visual estimates in surface >2 cm size fraction)
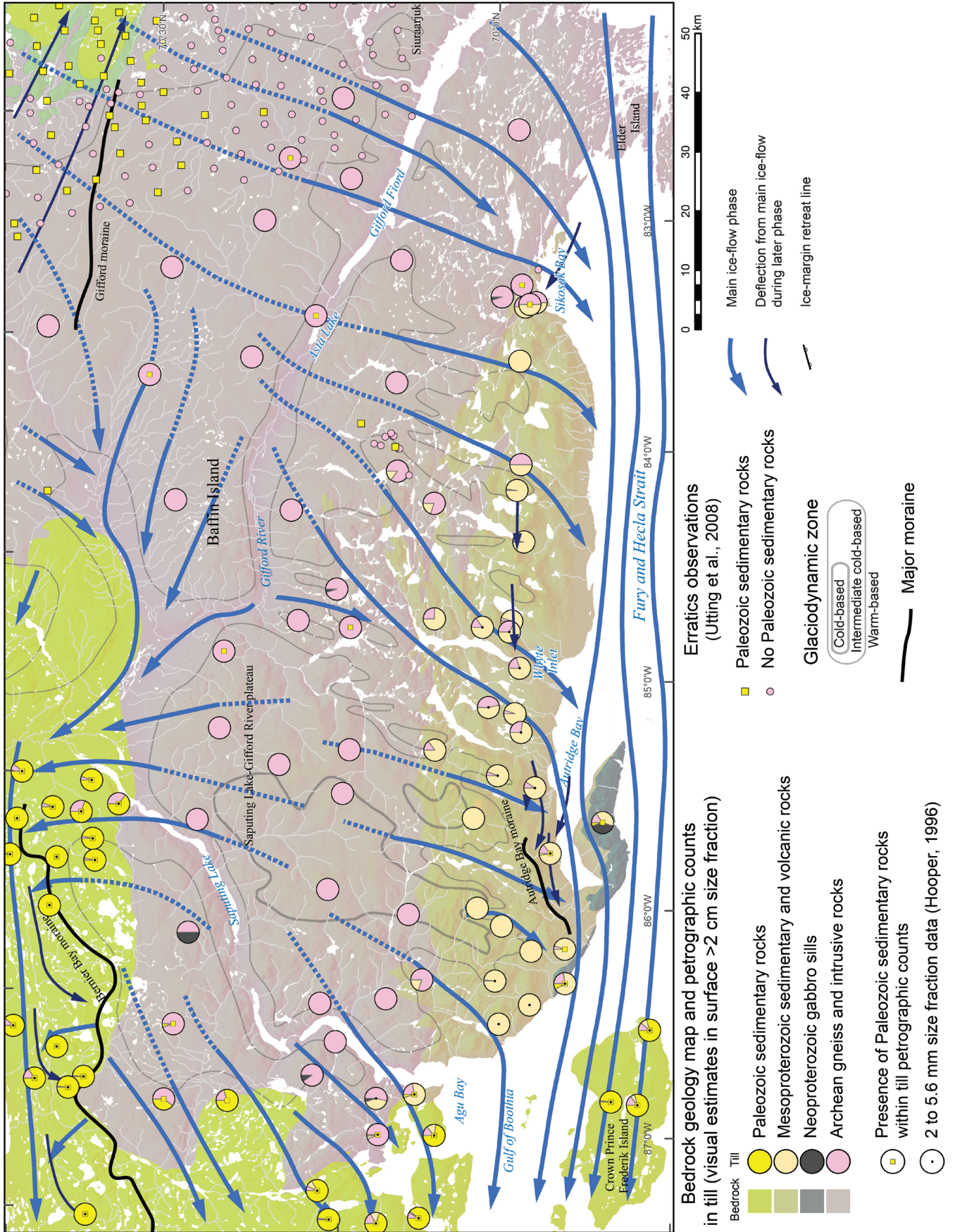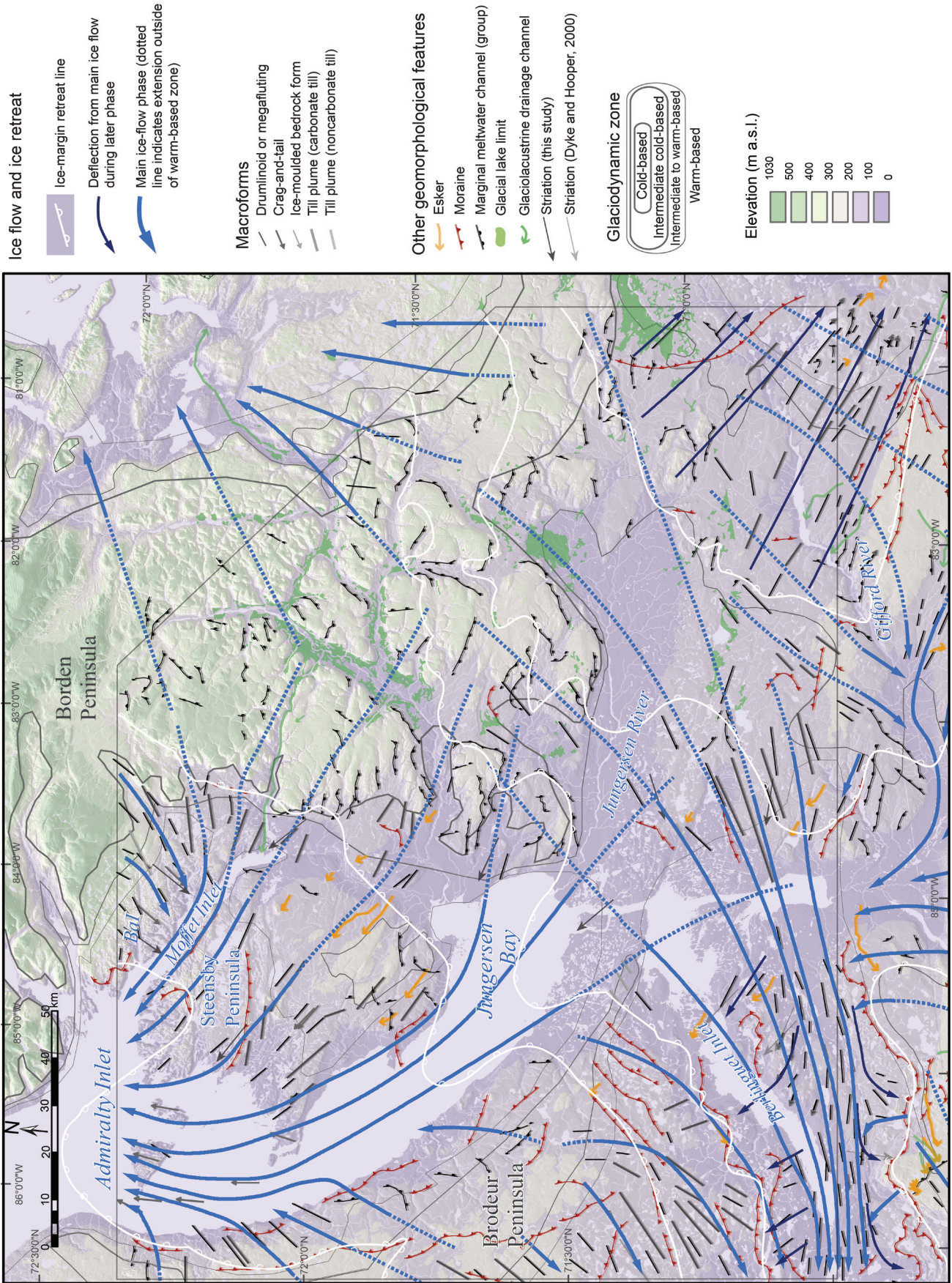
Figure 11. Ice-flow lines and ice-margin retreat lines with glacial geomorphology from the Jungersen River area (*from* Tremblay, 2021). Digital elevation model from Canadian digital elevation model (Natural Resources Canada, 2016). Study area outlined in grey.

South of Pond Inlet

Phases 1 and 2

Between Steensby Inlet and Milne Inlet (site M on Fig. 1), early north-northwest striations (Januszczak, 2007) and weak, but noticeable, glacial transport of Paleozoic carbonate rocks (Dyke, 2008) indicate early northward (north-northeast, north-northwest) ice flow toward Milne Inlet. East of Kapuiviit (formerly Jens Munk Island; site K on Fig. 1), the easternmost early striations (Dyke, 2008) and macroforms are oriented westward toward Fury and Hecla Strait. On the plateau east of Milne Inlet, early striations indicate north-northwest ice flow toward Paquet Bay (site P on Fig. 1; Little et al., 2004).

The ice-flow indicators described above are interpreted to have occurred during phase 1 and phase 2. There is no indication that ice-flow patterns would have varied much during the interval of the LGM and earliest deglaciation. The north-northwest striations reported by Januszczak (2007) and the westward striations by Dyke (2008) are interpreted as the inland limits of warm-based ice flow during phase 2. Hypothetically, during phase 1, these sites could have been cold-based. Over the area around Steensby Inlet and east of Kapuiviit, the conditions are inferred to have been mostly cold-based during phase 1 and phase 2. Carbonate erratics found east of Steensby Inlet (Andrews and Sim, 1964; Andrews and Miller, 1979; Dyke, 2008) indicate glacial transport during an indeterminate period, possibly during the LGM (phase 1) or pre-LGM times.

Phase 1 occurred during the LGM, and possibly prior to the LGM during late ice buildup, and phase 2 lasted from the LGM to about 9 ka, when ice margins in contact with the sea retreated to near the coastline around Milne Inlet.

Phase 3a

The phase 3a ice flow for most of the area south of Pond Inlet occurred in continuity with that from the northwestern Baffin Island region. Late ice flows toward a terrestrial margin are indicated by moraines, ice-marginal channels, eskers, and proglacial lake configurations (Dyke, 2000a, b). Late ice-flow events toward the north are also indicated by submarine moraines in the Tasiujaq (formerly Eclipse Sound) and Milne Inlet areas (Brouard and Lajeunesse, 2017), concordant with moraines related to northward flow on land (Klassen, 1993; Dyke, 2000a, b).

The phase 3a ice-flow pattern indicates a progressive, mostly cold-based retreat as the ice margin abandoned the last marine inlets and became fully terrestrial around 6 ka over the Steensby Inlet area, and earlier on the plateau around Gifford River (continuing terrestrial margin ice retreat from the northwestern Baffin Island area at 6.8 ka). Eventually, early Barnes Ice Cap features on central Baffin Island formed on the plateau around 6.8 ka. On the eastern highlands of Baffin Island, the ice retreated gradually toward the modern position of the Barnes Ice Cap and some of the other plateau ice caps (Dyke and Hooper, 2001; Gilbert et al., 2017), whereas retreat toward modern mountain glaciers might have occurred earlier in the Holocene (Margreth et al., 2014; Pendleton et al., 2019).

Phase 3b

Over the area around Steensby Inlet, later striations, macroforms, and glacial transport features indicate southeastward convergent–divergent ice flow toward Steensby Inlet and Kapuiviit (Steensby Inlet ice stream; Dyke, 2008). This ice flow was probably active during only a few centuries around 7 ka (Dyke, 2008). Near the ice divide between Milne Inlet and Steensby Inlet, southward striations crosscut earlier phase 2 north-northwestward striations (Januszczak, 2007). On Kapuiviit, late southwestward striations crosscut earlier striations trending westward toward Fury and Hecla Strait (phase 2; Dyke and Savelle, 2006; Dyke, 2008). Southward dispersal trains of Paleozoic sediments (carbonate and sandstone; Dyke and Savelle, 2006; Dyke, 2008; Utting et al., 2008) and KIMs (Januszczak, 2007) are observed in this area, and distances of glacial transport increase from the ice divide toward the coast, reflecting the increased velocity of ice flow toward the terminus of the ice stream.

Phase 3b corresponds to a brief but powerful ice-flow episode, commencing when the Steensby Inlet ice stream flowed south toward a glacial margin near the coast, south of Kapuiviit, until ice finally retreated north from Steensby Inlet (Dyke, 2008).

Northernmost Baffin Island

Phases 1 and 2

On northern Brodeur and Borden peninsulas, ice-flow indicators radiate outward from mostly cold-based terrains. Over these terrains, ice flowed from local ice divides,

independent of the rest of the LIS, and merged with ice streams in the deep marine channels (BLIS main axis, Admiralty Inlet, Navy Board Inlet, Tasiujaq, and Milne Inlet). Bathymetric data indicate macroforms along those marine channels as evidence for strong ice-stream flow (Bennett et al., 2016; Brouard and Lajeunesse, 2019). At the LGM, the ice flow toward Milne Inlet was channeled through Tasiujaq and Pond Inlet, toward Baffin Bay, joining with the BLIS in Baffin Bay. On Bylot Island and the area around Pond Inlet, the Eclipse till and Eclipse moraine formed at the margin of warm-based ice from regional ice flow depositing Paleozoic and Proterozoic sedimentary erratics. There are currently two opposing ideas for the age of the Eclipse moraine (and till). The first is a pre-LGM age based on stratigraphy, terrestrial cosmogenic nuclide surface-exposure dating of boulders, and stratigraphic correlations with radiocarbon- and amino-acid-dated units (Klassen, 1993; McCuaig, 1994); the landform was preserved under cold-based ice from the LGM to deglaciation. The second is an LGM age (Dyke and Hooper, 2001; Dyke et al., 2002) based on the Holocene age of the Navy Board Inlet moraine and the correlation of this moraine with the largest ice extent to occur during the entire Pleistocene (Dyke et al., 2002; Brouard and Lajeunesse, 2017).

In central Navy Board Inlet, a minor ice divide separated ice flowing toward the BLIS from glacial flow toward Tasiujaq. This ice-divide position is interpreted from a lack of glacial macroforms on the seafloor and the presence of the perfectly preserved pre-LGM Canada Point paleodelta on the shore of Navy Board Inlet (Fig. 3a; Klassen, 1993; Tremblay and Lamothe, 2019). After ice retreated from the adjacent Lancaster Sound, the divergent, down-ice portion of the northern Navy Board Inlet ice stream deposited moraines on both sides of the channel (Dyke and Hooper, 2001; Bennett et al., 2016). Phase 1 was active from late ice buildup to the LGM, and phase 2 progressively ended at about 10.9 ka, when most of the coastline was deglaciated.

Phase 3

As the ice gradually retreated from inland, the orientation of moraines, marginal channels, and proglacial lake configurations indicates that the ice front was retreating in a concentric pattern, with cold-based ice flowing quasi-radially, with twists and deviations occurring according to local topographic peculiarities (Dyke and Hooper, 2001).

During this phase, cold-based ice, and locally polythermal valley glaciers, retreated toward modern glaciers and ice caps on Brodeur Peninsula, Borden Peninsula, Bylot Island, and near the southern coast of Pond Inlet.

DISCUSSION

Relative ice-flow chronology data and possible reconstructions

Although a reconstruction of three main ice-flow phases was produced from a synthesis of regional ice-flow histories for the BLIS catchment area, given the fragmented and poorly time-constrained nature of the data, it follows that different interpretations can be applied to the various ice-flow data sets. By nature, the ice-flow record is more spatially continuous for macroforms and discontinuous for striations, and for both, some of the record may have been removed due to erosion by subsequent ice-flow events or covered by later sedimentary sequences. Therefore, the older the striae set (or other paleoflow indicator), the more the interpretation can vary, in part because of the impossibility of dating glacial striations using absolute methods. For example, as an outcome of this drawback, it could be argued that the older, northward striations south of Boothia Isthmus, part of phase 1 and tentatively assigned to the LGM, could alternatively be attributed to pre-LGM glaciation(s). In this scenario, phase 2 would have started at the LGM instead of during deglaciation. Throughout this synthesis, although efforts have been made to present the most coherent interpretation using all available data, alternative interpretations are impossible to dismiss entirely. Ultimately, because multiple solutions are likely to result from multiscale, truncated data sets, there is a need for a data-compilation platform that will allow evaluation of data sets, comparison of different scenarios, and the assessment of the magnitude of the uncertainty for each proposed reconstruction. Such a structured data platform, in which multiple-scale glacial data sets could be consolidated for analysis, was recently developed for a large region west of Hudson Bay in Nunavut that includes the southwestern part of the BLIS catchment area (Behnia et al., 2020; McMartin et al., 2021). Expansion of this glacial data platform to include the entire BLIS-area data sets offers the capacity to process multiple interpretations and could be useful in the production of different working hypotheses in glacial modelling and for future fieldwork.

New implications for NELIS dynamics

New evidence for both stability and fluctuations in the intensity and patterns of ice flow is presented and evaluated in the BLIS catchment area. Building on glacial reconstructions of the LGM to deglaciation, such as those of Dyke and Prest (1987a), Dyke and Hooper (2001), De Angelis (2007a), and Margold et al. (2018), the synthesis of field data and new mapping on land and offshore shows that convergent high-velocity ice flows through the BLIS main axis was a

major, persistent feature in the NELIS throughout the Late Wisconsinan glaciation. As the ice-flow velocities changed (i.e. generally increased) from the LGM to deglaciation, the patterns of ice flow were transformed, reflecting the channelling of ice toward varying regional topographic lows connected to the deep depression occupied by the BLIS. New tributary ice streams are recognized (FBIS, FHIS, GBIS, JBIS, LMIS, MOIS, WIIS), and different names for previously established ice streams (BIIS, BLIS, BSIS) are proposed to better reflect their location and extent from the LGM until deglaciation.

The data and interpretations presented in this study have implications for glaciodynamic constraints on ice flows, as expressed by the updated mapping of low-velocity zones in cold-based landscapes and high-velocity zones in ice streams. Several recent field studies on the high plateaus of southeastern Baffin Island (Johnson et al., 2013; Tremblay et al., 2016a), Melville Peninsula (Tremblay and Paulen, 2012), and Wager Bay (McMartin et al., 2021) showed that the transition from warm-based to cold-based glacial landscapes generally appears to be gradational over a zone several tens of kilometres in width. The incremental impact of spatially variable subglacial thermal conditions over time is probably the cause of these subtle transition zones.

Numerous striation and till-clast data have led to an improved understanding of successive ice flows in the BLIS catchment area, particularly on the mainland portion of the western part of this area. Notably, variable ice-flow patterns and palimpsest glacial transport dispersal trains were identified south of Boothia Isthmus to the KID that would have formed during the LGM (phase 1) until early deglaciation (phase 2). Phase 1 switched to phase 2 in this area because ice flow accelerated within the BLIS main axis, enlarging the footprint of the Boothia Isthmus ice stream and depressing the ice profile, thus speeding up ice flow within the region. As a result, the catchment area of the BLIS may have been larger during phase 2 relative to phase 1 (for example on southern Melville Peninsula). North of Boothia Isthmus, the presence of carbonate erratics in the core zone of the cold-based plateau confirmed that a weak, but discernible, glacial transport occurred under cold-based ice-flow conditions. On Melville Peninsula, precise mapping of a late deglaciation ice-flow reversal during phase 3 was determined from new striae, macroforms, and pebble data. On the southern part of this peninsula, new data on the distribution of Paleozoic carbonate clasts in till indicated a possible local source for those clasts on the southeastern shores, which suggests that ice did not cross over from Foxe Basin and farther west into Committee Bay.

To the east beyond Nunavut's mainland, understanding of ice-flow patterns has also improved. In the region straddling Baffin Island and Melville Peninsula, evidence has shown that the Autridge Bay moraine and the northern Melville moraine were part of an end moraine formed during retreat of the ice-stream system in the Fury and Hecla Strait (FHIS), as opposed to being the limit of ice flow descending south from the hills located north of the Fury and Hecla Strait (Dyke and Prest, 1987b; Dredge, 2001). In the central part of Navy Board Inlet, new bathymetric data sets showed the absence of macroforms on till surface, as well as the presence of a pristine pre-LGM delta close to the shoreline, indicating lasting flow separation and cold-based ice conditions under a subsidiary ice divide (Fig. 3a).

Warm-based interior of the NELIS?

The data synthesized here suggest that ice streams in the NELIS were active during the LGM until deglaciation. This work also presents new evidence for the absence of ice flowing northward over the cold-based Saputing Lake–Gifford River plateau on Baffin Island during the LGM and possibly during pre-LGM glaciations. This evidence provides clear support for glacial reconstructions (Dyke and Prest, 1987b; De Angelis, 2007a; Margold et al., 2018) in which westward ice streaming in the Fury and Hecla Strait and northern Melville Peninsula, feeding an important inner core of the BLIS catchment area, was prevalent during the LGM and until deglaciation of marine-based ice margins (10.3 ka). In the southwestern part of the BLIS catchment area, south of the study area, glacial stratigraphy, till provenance, and mapping of glacial landsystems suggest that ice streams might have reached the interior of the KD during the marine-based ice-margin deglaciation phase of the BLIS (Hodder et al., 2016; McMartin et al., 2021). These assertions deal with the important paleoglaciological question of whether warm-based ice flow extended into the interior of the NELIS during the LGM and early deglaciation or cold-based conditions prevailed. In the work presented here, although cold-based landscapes were recognized over high plateaus and under former ice divides, most evidence points toward a well developed ice-stream network being active during the last glaciation. This warm-based interior of the NELIS is consistent with reconstructions presented by Dyke and Prest (1987a, b), De Angelis (2007a), Stokes et al. (2012), and Margold et al. (2018) but presents a slightly more extended footprint of auxiliary ice-stream activity within the BLIS catchment area during the LGM. The contrasting view outlined in Kleman and Glasser (2007), whereby warm-based ice flows could be highly diachronic, occurring only on the outer rims of ice sheets, and the northern Laurentide Ice Sheet was mostly cold-based during the LGM, is not supported by the evidence presented here.

Future work

This study is a first step in the synthesis of ice-flow indicators observed around Foxe Basin and Baffin Island in a large part of the BLIS catchment area, focusing especially on striations, macroforms, and glacial transport of Paleozoic carbonate erratics. The reconstruction of the three ice-flow phases presented here is certainly limited and could be expanded

into more time slices and greater detail using appropriate and more complete data sets. For example, in the area around Steensby Inlet, the full picture of the successive ice flows was not captured in this generalized reconstruction. Other regions also deserve closer scrutiny, including Pelly Bay, where new bathymetric, till composition, and striae data sets suggest a much more complex series of events than those depicted here. Similarly, although new evidence on the floor of Peel Sound is constraining the provenance of carbonate clasts in the Bellot Strait area to a closer source, the complexity of cold-based and warm-based ice flows around Prince of Wales Island, Peel Sound, and Bellot Strait needs to be re-examined in detail.

In many other areas, additional field data sets would help increase the resolution of the glacial reconstructions. Late during deglaciation, local topography played an increasingly important role in the dynamics of ice draining into the marine troughs in and around Chantrey Inlet, Rasmussen Basin, Adelaide Peninsula, and King William Island. Relatively pronounced changes in ice-flow directions occurred within short distances in these regions, compared to surrounding, flatter terrains on land. New fieldwork around this region, where the ice-flow record is scarce (Prest et al., 1968), could provide key elements for the ice-stream chronology in the western BLIS catchment sector. In addition to increasing the ice-flow record, the regional stratigraphic context of the entire BLIS catchment area needs to be updated, notably with new geochronological measurements (terrestrial cosmogenic nuclide, infrared-stimulated luminescence) in the northeastern Baffin Island and Bylot Island sectors (Klassen, 1993; Tremblay et al., 2020a). The age of the Eclipse moraine, in particular, is a major issue that warrants further study.

Finally, numerical ice-sheet modelling experiments could attempt to reproduce the ice-flow phases proposed here. For example, the models could try to account for the ice-flow pattern variability in the area between Boothia Isthmus and the KID, as well as between Boothia Peninsula and the MID, and for the absence of north or northwest ice flows over the Saputing Lake–Gifford River plateau. In Stokes et al. (2012), the modelled ice flow from 65 to 25 ka generally shows a northwest ice-flow direction over the Saputing Lake–Gifford River plateau and Fury and Hecla Strait, which contradicts the petrographic study of till clasts in this area (Tremblay and Godbout, 2018). To solve this disagreement, the model could extend areas of enhanced basal sliding to regions where ice-stream footprints were mapped, including over northern Melville Peninsula (a mostly hard-bedded ice stream in this case) and Fury and Hecla Strait.

CONCLUSION

Regional ice-flow patterns and chronology were reconstructed in the BLIS catchment area by synthesizing results and interpretations from previous work and from new striation measurements, glacial transport studies, and macroform

mapping using ArcticDEM, satellite images, and multibeam bathymetric data. Three main ice-flow phases were reconstructed:

- phase 1: active ice flow within the BLIS, at the LGM

- phase 2: increasingly active and far-reaching ice flow within the BLIS, between the LGM and 10.3 ka

- phase 3: local ice flows in various tributary ice-stream catchment areas, toward retreating terrestrial or coastal ice margins after 10.3 ka.

Generally, the synthesized field data support the presence of ice streams and variable ice-flow patterns, which are generally in accord with most recent reconstructions primarily based on remote sensing (De Angelis, 2007a; Margold et al., 2018). However, the results from this study suggest that the footprints of auxiliary ice streams within the BLIS catchment area were slightly more extended during deglaciation (phase 2) than during the LGM (phase 1). More importantly, new bathymetric observations on the seafloor of major depressions bring fresh elements to the ice-flow history. In the BLIS main axis, seafloor geomorphological interpretations indicate a strong continuity of macroforms from Prince Regent Inlet to Lancaster Sound; the continuity is much less apparent from Barrow Strait to Lancaster Sound, probably because the ice flow between Barrow Strait and Lancaster Sound was volumetrically less important than that from Prince Regent Inlet to Lancaster Sound. Between Committee Bay and Prince Regent Inlet, the seafloor data indicate the continuity of macroforms, interpreted as marking the footprint of the BLIS. Also, new seabottom morphology evidence indicates that a cold-based ice divide was situated within Navy Board Inlet between Bylot and Baffin islands. The mapping of cold-based glacial landscapes is also a key element in the proposed reconstruction of glacial dynamics and ice-flow events. In many regions, this compilation can be used as a tool to study changes in glacial transport and glacial patterns during the last glaciation.

An integrated GIS-based data platform is necessary to combine and make accessible field data and remote-sensing data, used to test and strengthen competing glacial flow reconstructions, especially for the early pre-LGM phases, where evidence of older ice flows is equivocal. Glacial modelling studies can use the glacial history interpretations presented here as a driver for refining the constraints on ice-flow chronology and patterns in different geographic settings and at different times. In turn, the numerical models can provide feedback on the processes at work in the BLIS catchment area and in the NELIS in general.

ACKNOWLEDGMENTS

REFERENCES

Andrews, J.T., 1989. Quaternary Geology of the northeastern Canadian Shield; Chapter 3 *in* Quaternary geology of Canada and Greenland, (ed.) R.J. Fulton; Geological Survey of Canada, Geology of Canada, no. 1, p. 276–307 (also Geological Society of America, The geology of North America, v. K-1, p. 276–307). https://doi.org/10.4095/127975

Andrews, J.T. and Miller, G.H., 1979. Glacial erosion and ice sheet divides, northeastern Laurentide Ice Sheet, on the basis of the distribution of limestone erratics; Geology, v. 7, no. 12, p. 592–596. https://doi.org/10.1130/0091-7613(1979)7%3c592:GEAISD%3e2.0.CO%3b2

Andrews, J.T. and Peltier, W.R., 1989. Introduction — Quaternary geodynamics in Canada; Chapter 8 *in* Quaternary geology of Canada and Greenland, (ed.) R.J. Fulton; Geological Survey of Canada, Geology of Canada, no. 1, p. 543–572 (also Geological Society of America, The geology of North America, v. K-1, p. 543–572). https://doi.org/10.4095/131626

Andrews, J.T. and Sim, V.W., 1964. Examination of the carbonate content of drift in the area of Foxe Basin, N.W.T.; Geographical Bulletin, v. 21, p. 44–53.

Andrews, J.T., Clark, P., and Stravers, J., 1985. The pattern of glacial erosion across the eastern Canadian Arctic; *in* Quaternary environments: eastern Canadian Arctic, Baffin Bay and west Greenland, (ed.) J.T. Andrews; Allen and Unwin, Winchester, Massachusetts, p. 69–92.

Andrews, J.T., Kirby, M.E., Aksu, A., Barber, D.C., and Meese, D., 1998. Late Quaternary detrital carbonate (DC-) layers in Baffin Bay marine sediments (67°–74°N): correlation with Heinrich events in the North Atlantic?; Quaternary Science Reviews, v. 17, no. 12, p. 1125–1137. https://doi.org/10.1016/S0277-3791(97)00064-4

Andrews, J.T., Gibb, O.T., Jennings, A.E., and Simon, Q., 2014. Variations in the provenance of sediment from ice sheets surrounding Baffin Bay during MIS 2 and 3 and export to the Labrador Shelf Sea: site HU2008029-0008 Davis Strait; Journal of Quaternary Science, v. 29, no. 1, p. 3–13. https://doi.org/10.1002/jqs.2643

Behnia, P., McMartin, I., Campbell, J.E., Godbout, P.-M., and Tremblay, T., 2020. Northern Canada glacial geomorphology database: part 1 — central mainland Nunavut; Geological Survey of Canada, Open File 8717, 6 p. https://doi.org/10.4095/327796

Bennett, R., Campbell, D.C., and Furze, M.F.A., 2014. The shallow stratigraphy and geohazards of the northeast Baffin Shelf and Lancaster Sound; Bulletin of Canadian Petroleum Geology, v. 62, no. 4, p. 217–231. https://doi.org/10.2113/gscpgbull.62.4.217

Bennett, R., Maclean, B., Blasco, S., and Clarke, J.H., 2016. Glacial lineations in Navy Board Inlet, Nunavut, Canada; Geological Society of London, Memoirs, v. 46, p. 49–50.

Bonham-Carter, G., Peter, J.M., Corrigan, D., Day, S.J.A., McClenaghan, M.B., McNeil, R.J., Tremblay, T., and Garrett, R.G., 2019. Lake sediment geochemical evaluation of the mineral potential of west-central Baffin Island, Nunavut; Geological Survey of Canada, Open File 8590, 70 p. https://doi.org/10.4095/321091

Boulton, G.S. and Clark, C.D., 1990. A highly mobile Laurentide ice sheet revealed by satellite images of glacial lineations; Nature, v. 346, p. 813–817. https://doi.org/10.1038/346813a0

Brouard, É. and Lajeunesse, P., 2017. Maximum extent and decay of the Laurentide Ice Sheet in western Baffin Bay during the last glacial episode; Scientific Reports, v. 7, no. 1, art. no. 10711. https://doi.org/10.1038/s41598-017-11010-9

Brouard, É. and Lajeunesse, P., 2019. Submarine geomorphology of the northeastern Baffin Island fiords and cross-shelf troughs; Journal of Maps, v. 15, no. 2, p. 662–676. https://doi.org/10.1080/17445647.2019.1647302

Clark, C.D. and Stokes, C.R., 2001. Extent and basal characteristics of the M'Clintock Channel ice stream; Quaternary International, v. 86, no. 1, p. 81–101. https://doi.org/10.1016/S1040-6182(01)00052-0

Clark, P.U., Dyke, A.S., Shakun, J.D., Carlson, A.E., Clark, J., Wohlfarth, B., Mitrovica, J.X., Hostetler, S.W., and McCabe, A.M., 2009. The last glacial maximum; Science, v. 325, no. 5941, p. 710–714. https://doi.org/10.1126/science.1172873

Dalton, A.S., Margold, M., Stokes, C.R., Tarasov, L., Dyke, A.S., Adams, R.S., Allard, S., Arends, H.E., Atkinson, N., Attig, J.W., Barnett, P.J., Barnett, R.L., Batterson, M., Bernatchez, P., Borns, H.W., Jr., Breckenridge, A., Briner, J.P., Brouard, É., Campbell, J.E., . . . Wright, H.E., Jr., 2020. An updated radiocarbon-based ice margin chronology for the last deglaciation of the North American ice sheet complex; Quaternary Science Reviews, v. 234, art. no. 106223. https://doi.org/10.1016/j.quascirev.2020.106223

De Angelis, H., 2007a. Palaeo-ice streams in the north-eastern Laurentide Ice Sheet; Ph.D. thesis, Stockholm University, Stockholm, Sweden, 123 p.

De Angelis, H., 2007b. Glacial geomorphology of the east-central Canadian Arctic; Journal of Maps, v. 3, p. 323–341. https://doi.org/10.1080/jom.2007.9710848

De Angelis, H. and Kleman, J., 2005. Palaeo-ice streams in the northern Keewatin sector of the Laurentide ice sheet; Annals of Glaciology, v. 42, p. 135–144. https://doi.org/10.3189/172756405781812925

De Angelis, H. and Kleman, J., 2007. Palaeo-ice streams in the Foxe/Baffin sector of the Laurentide Ice Sheet; Quaternary Science Reviews, v. 26, p. 1313–1331. https://doi.org/10.1016/j.quascirev.2007.02.010

de Kemp, E.A. and Scott, D.J., 1998. Geoscience compilation of northern Baffin Island and northern Melville Peninsula, Northwest Territories; Geological Survey of Canada, Open File 3636, 2 CD-ROMs. https://doi.org/10.4095/210027

de Kemp, E.A., Gilbert, C., and James, D.T., 2006. Geology of Nunavut; Geological Survey of Canada–Canada-Nunavut Geoscience Office, scale 1:3 500 000. <http://cngo.ca/content/uploads/geology_of_nunavut.pdf> [accessed August 2018]

Denton, G.H. and Hughes, T.J. (ed.), 1981. The last great ice sheets; Wiley, New York, 484 p.

Dredge, L.A., 1995. Quaternary geology of northern Melville Peninsula, District of Franklin, Northwest Territories: surface deposits, glacial history, environmental geology, and till geochemistry; Geological Survey of Canada, Bulletin 484, 114 p. https://doi.org/10.4095/205729

Dredge, L.A., 2000. Age and origin of upland block fields on Melville Peninsula, eastern Canadian Arctic; Geografiska Annaler, v. 82, no. 4, p. 443–454. https://doi.org/10.1111/j.0435-3676.2000.00133.x

Dredge, L.A., 2001. Late Pleistocene and Holocene glaciation and deglaciation of Melville Peninsula, northern Laurentide Ice Sheet; Géographie physique et Quaternaire, v. 55, no. 2, p. 159–170. https://doi.org/10.7202/008300ar

Dredge, L.A., 2002. Quaternary geology of southern Melville Peninsula, Nunavut; Geological Survey of Canada, Bulletin 561, 110 p. https://doi.org/10.4095/213215

Dredge, L.A., 2004. Till geochemistry results, central Baffin Island, Nunavut (NTS 37A, 37D, 27B, 27C); Geological Survey of Canada, Open File 4543, 1 .zip file. https://doi.org/10.4095/214996

Dyke, A.S., 1984a. Surficial geology, Somerset Island, District of Franklin, Northwest Territories; Geological Survey of Canada, Map 1555A, scale 1:250 000. https://doi.org/10.4095/119720

Dyke, A.S., 1984b. Quaternary geology of Boothia Peninsula and northern District of Keewatin, central Canadian Arctic; Geological Survey of Canada, Memoir 407, 26 p. https://doi.org/10.4095/119731

Dyke, A.S., 1993. Landscapes of cold-centred Late Wisconsinan ice caps, Arctic Canada; Progress in Physical Geography, v. 17, no. 2, p. 223–247. https://doi.org/10.1177/030913339301700208

Dyke, A.S., 2000a. Surficial geology, Milne Inlet, Baffin Island, Nunavut; Geological Survey of Canada, Map 1962A, scale 1:250 000. https://doi.org/10.4095/211528

Dyke, A.S., 2000b. Surficial geology, Phillips Creek, Baffin Island, Nunavut; Geological Survey of Canada, Map 1961A, scale 1:250 000. https://doi.org/10.4095/211526

Dyke, A.S., 2008. The Steensby Inlet ice stream in the context of the deglaciation of northern Baffin Island, eastern Arctic Canada; Earth Surface Processes and Landforms, v. 33, p. 573–592. https://doi.org/10.1002/esp.1664

Dyke, A.S. and Dredge, L.A., 1989. Quaternary geology of the northwestern Canadian Shield; Chapter 3 in Quaternary geology of Canada and Greenland, (ed.) R.J. Fulton; Geological Survey of Canada, Geology of Canada, no. 1, p. 189–214 (also Geological Society of America, The geology of North America, v. K-1, p. 189–214). https://doi.org/10.4095/127963

Dyke, A.S. and Evans, D.J.A., 2003. Ice-marginal terrestrial landsystems: northern Laurentide and Innuitian ice sheet margins; Chapter 7 in Glacial landsystems, (ed.) D.J.A. Evans; Arnold, London, United Kingdom, p. 143–165. https://doi.org/10.4324/9780203784976

Dyke, A.S. and Hooper, J.M.G., 2000. Till geochemistry, Borden and Brodeur peninsulas of northern Baffin Island and Devon Island; Geological Survey of Canada, Open File 3907, 15 p. https://doi.org/10.4095/211487

Dyke, A.S. and Hooper, J.M.G., 2001. Deglaciation of northwest Baffin Island, Nunavut; Geological Survey of Canada, Map 1999A, scale 1:500 000. https://doi.org/10.4095/212484

Dyke, A.S. and Matthews, J.V., 1987. Stratigraphy and paleoecology of Quaternary sediments exposed along Pasley River, Boothia Peninsula, central Canadian Arctic; Géographie physique et Quaternaire, v. 41, no. 3, p. 323–344. https://doi.org/10.7202/032689ar

Dyke, A.S. and Morris, T.F., 1988. Drumlin fields, dispersal trains, and ice streams in Arctic Canada; The Canadian Geographer / Le Géographe canadien, v. 32, no. 1, p. 86–90.

Dyke, A.S. and Prest, V.K., 1987a. Late Wisconsinan and Holocene history of the Laurentide Ice Sheet; Géographie physique et Quaternaire, v. 41, p. 237–263. https://doi.org/10.7202/032681ar

Dyke, A.S. and Prest, V.K., 1987b. Paleogeography of northern North America, 18 000–5000 years ago; Geological Survey of Canada, Map 1703A, scale 1:5 000 000. https://doi.org/10.4095/133927

Dyke, A.S. and Savelle, J.M., 2006. Surficial geology, southwest Jens Munk Island, Nunavut; Geological Survey of Canada, Open File 4954, scale 1:50 000. https://doi.org/10.4095/223018

Dyke, A.S., Andrews, J.T., and Miller, G.H., 1982. Quaternary geology of Cumberland Peninsula, Baffin Island, District of Franklin; Geological Survey of Canada, Memoir 403, 32 p. https://doi.org/10.4095/116169

Dyke, A.S., Morris, T.F., Green, D.E.C., and England, J., 1992. Quaternary geology of Prince of Wales Island, Arctic Canada; Geological Survey of Canada, Memoir 433, 149 p. https://doi.org/10.4095/134058

Dyke, A.S., Andrews, J.T., Clark, P.U., England, J.H., Miller, G.H., Shaw, J., and Veillette, J.J., 2002. The Laurentide and Innuitian ice sheets during the last glacial maximum; Quaternary Science Reviews, v. 21, no. 1-3, p. 9–31. https://doi.org/10.1016/S0277-3791(01)00095-6

Dyke, A.S., Moore, A., and Robertson, L., 2003. Deglaciation of North America; Geological Survey of Canada, Open File 1574, 1 CD-ROM, scale 1:30 000 000. https://doi.org/10.4095/214399

Dyke, A.S., Dredge, L.A., and Hodgson, D.A., 2005. North American deglacial marine- and lake-limit surfaces; Géographie physique et Quaternaire, v. 59, no. 2-3, p. 155–185. https://doi.org/10.7202/014753ar

England, J., Atkinson, N., Bednarski, J., Dyke, A.S., Hodgson, D.A., and Ó Cofaigh, C., 2006. The Innuitian Ice Sheet: configuration, dynamics and chronology; Quaternary Science Reviews, v. 25, no. 7-8, p. 689–703. https://doi.org/10.1016/j.quascirev.2005.08.007

England, J.H., Furze, M.F.A., and Doupé, J.P., 2009. Revision of the NW Laurentide Ice Sheet: implications for paleoclimate, the northeast extremity of Beringia, and Arctic Ocean sedimentation; Quaternary Science Reviews, v. 28, no. 17-18, p. 1573–1596. https://doi.org/10.1016/j.quascirev.2009.04.006

Fulton, R.J., 1995. Surficial materials of Canada / Matériaux superficiels du Canada; Geological Survey of Canada, Map 1880A, scale 1:5 000 000. https://doi.org/10.4095/205040

Giangioppi, M., Little, E.C., Ferbey, T., Ozyer, C.A., and Utting, D.A., 2003. Quaternary glaciomarine environments west of Committee Bay, central mainland Nunavut; Geological Survey of Canada, Current Research 2003-C5, 12 p. https://doi.org/10.4095/214187

Gilbert, A., Flowers, G.E., Miller, G.H., Refsnider, K.A., Young, N.E., and Radić, V., 2017. The projected demise of Barnes Ice Cap: evidence of an unusually warm 21st century Arctic; Geophysical Research Letters, v. 44, no. 6, p. 2810–2816. https://doi.org/10.1002/2016GL072394

Helie, R.G., 1984. Surficial geology, King William Island and Adelaide Peninsula, districts of Keewatin and Franklin, Northwest Territories; Geological Survey of Canada, Map 1618A, scale 1:250 000. https://doi.org/10.4095/120012

Hodder, T.J., Ross, M., and Menzies, J., 2016. Sedimentary record of ice divide migration and ice streams in the Keewatin core region of the Laurentide Ice Sheet; Sedimentary Geology, v. 338, p. 97–114. https://doi.org/10.1016/j.sedgeo.2016.01.001

Hooper, J.M.G., 1996. Glacial history and Holocene sea level regression in the Foxe/Baffin sector of the Laurentide Ice Sheet, northwest Baffin Island, Arctic Canada; Ph.D. thesis, University of Alberta, Edmonton, Alberta, 195 p.

Ives, J.D. and Andrews, J.T., 1963. Studies in the physical geography of north-central Baffin Island; Geographical Bulletin, v. 19, p. 5–48.

Januszczak, N., 2007. Glacial geology: Baffin Island project 2006; in Assessment report on the 2006 prospecting, mapping, geophysics and drill programmes on the Baffin property, Nunavut, De Beers Canada Inc., (ed.) B. McMonnies, J. McKenzie, N. Januszczak, and D. Chartier; Indigenous and Northern Affairs Canada, Assessment Report 085113, 123 p.

Johnson, C., Ross, M., and Tremblay, T., 2013. Glacial geomorphology of north-central Hall Peninsula, southern Baffin Island; Geological Survey of Canada, Open File 7413, 56 p. https://doi.org/10.4095/293037

Klassen, R.A., 1993. Quaternary geology and glacial history of Bylot island, Northwest Territories; Geological Survey of Canada, Memoir 429, 93 p. https://doi.org/10.4095/183984

Kleman, J. and Glasser, N.F., 2007. The subglacial thermal organisation (STO) of ice sheets; Quaternary Science Reviews, v. 26, no. 5-6, p. 585–597. https://doi.org/10.1016/j.quascirev.2006.12.010

Kleman, J., Hättestrand, C., Stroeven, A.P., Jansson, K.N., De Angelis, H., and Borgström, I., 2006. Reconstruction of palaeo-ice sheets — inversion of their glacial geomorphological record; Chapter 38 in Glacier science and environmental change, (ed.) P.G. Knight; Blackwell Publishing, p. 192–198. https://doi.org/10.1002/9780470750636.ch38

Kupsch, B. and Armstrong, J.P., 2013. Exploration and geology of the Qilalugaq kimberlites, Rae Isthmus, Nunavut, Canada; in Proceedings of 10th International Kimberlite Conference, Volume 2, (ed.) D.G. Pearson, H.S. Grütter, J.W. Harris, B.A. Kjarsgaard, H. O'Brien, N.V.C. Rao, and S. Sparks; Springer, New Delhi, p. 67–78. https://doi.org/10.1007/978-81-322-1173-0_5

Leblanc-Dumas, J., Allard, M., and Tremblay, T., 2014. Pre or interglacial regolith persistence under non-erosive ice during last glacial maximum in central Hall Peninsula, Baffin Island, Nunavut, Canada; GAC–MAC Joint Annual Meeting: Geological Association of Canada–Mineralogical Association of Canada, Abstracts, v. 37, p. 156.

Leblanc-Dumas, J., Allard, M., and Tremblay, T., 2015. Characteristics of a preglacial or interglacial regolith preserved under nonerosive ice during the last glacial maximum in central Hall Peninsula, southern Baffin Island, Nunavut; in Summary of activities 2014; Canada-Nunavut Geoscience Office, p. 69–78.

Lee, H.A., Craig, B.G., and Fyles, J.G., 1957. Keewatin ice divide; Geological Society of America Bulletin, v. 68, p. 1760–1761.

Li, G., Piper, D.J.W., and Campbell, D.C., 2011. The Quaternary Lancaster Sound trough-mouth fan, NW Baffin Bay; Journal of Quaternary Science, v. 26, no. 5, p. 511–522. https://doi.org/10.1002/jqs.1479

Little, E., 2001. Preliminary results of relative ice-movement chronology of the Laughland Lake map area, Nunavut; Geological Survey of Canada, Current Research 2001-C14, 7 p. https://doi.org/10.4095/212092

Little, E.C., Holme, P.J., Hilchey, A.C., and Young, M., 2004. Glacial geology, ice-movement chronology, and drift prospecting in the vicinity of Icebound Lakes, northern Baffin Island, Nunavut; Geological Survey of Canada, Current Research 2004-B1, 16 p. https://doi.org/10.4095/215103

Margold, M., Stokes, C.R., Clark, C.D., and Kleman, J., 2015. Ice streams in the Laurentide Ice Sheet: a new mapping inventory; Journal of Maps, v. 11, p. 380–395. https://doi.org/10.1080/17445647.2014.912036

Margold, M., Stokes, C.R., and Clark, C.D., 2018. Reconciling records of ice streaming and ice margin retreat to produce a palaeogeographic reconstruction of the deglaciation of the Laurentide Ice Sheet; Quaternary Science Reviews, v. 189, p. 1–30. https://doi.org/10.1016/j.quascirev.2018.03.013

Margreth, A., Dyke, A.S., Gosse, J.C., and Telka, A.M., 2014. Neoglacial ice expansion and late Holocene cold-based ice cap dynamics on Cumberland Peninsula, Baffin Island, Arctic Canada; Quaternary Science Reviews, v. 91, p. 242–256. https://doi.org/10.1016/j.quascirev.2014.02.005

Margreth, A., Gosse, J.C., and Dyke, A.S., 2016. Quantification of subaerial and episodic subglacial erosion rates on high latitude upland plateaus: Cumberland Peninsula, Baffin Island, Arctic Canada; Quaternary Science Reviews, v. 133, p. 108–129. https://doi.org/10.1016/j.quascirev.2015.12.017

Marsella, K.A., Bierman, P.R., Thompson Davis, P., and Caffee, M.W., 2000. Cosmogenic ^{10}Be and ^{26}Al ages for the last glacial maximum, eastern Baffin Island, Arctic Canada; Geological Society of America Bulletin, v. 112, no. 8, p. 1296–1312. https://doi.org/10.1130/0016-7606(2000)112%3c1296:CBAAAF%3e2.0.CO%3b2

Mayewski, P.A., Denson, G.H., and Hughes, T.J., 1981. Late Wisconsin ice sheets in North America; in The last great ice sheets, (ed.) G.H. Denton and T.J. Hughes; Wiley, New York, p. 67–178.

McCuaig, S.J., 1994. Glacial chronology of the south Bylot and Salmon River lowlands, NWT, using erratic dispersal patterns, cosmogenic dating, radiocarbon dating and lichenometry; M.Sc. thesis, Carleton University, Ottawa, Ontario, 140 p.

McMartin, I. and Dredge, L., 2005. History of ice flow in the Shultz Lake and Wager Bay areas, Kivalliq region, Nunavut; Geological Survey of Canada, Current Research 2005-B2, 10 p. https://doi.org/10.4095/220376

McMartin, I. and Henderson, P.J., 2004. Evidence from Keewatin (central Nunavut) for paleo-ice divide migration; Géographie physique et Quaternaire, v. 58, no. 2-3, p. 163–186. https://doi.org/10.7202/013137ar

McMartin, I., Utting, D.J., Little, E.C., Ozyer, C.A., and Ferbey, T., 2003. Complete results from the Committee Bay drift prospecting survey, central Nunavut; Geological Survey of Canada, Open File 4493, 1 .zip file. https://doi.org/10.4095/214646

McMartin, I., Campbell, J.E., Dredge, L.A., LeCheminant, A.N., McCurdy, M.W., and Scromeda, N., 2015. Quaternary geology and till composition north of Wager Bay, Nunavut: results from the GEM Wager Bay Surficial Geology project; Geological Survey of Canada, Open File 7748, 53 p. https://doi.org/10.4095/296419

McMartin, I., Tremblay, T., and Godbout, P.-M., 2017. Report of 2017 field activities for the GEM-2 Rae glacial history activity in the Kivalliq region, Nunavut; Geological Survey of Canada, Open File 8320, 14 p. https://doi.org/10.4095/306006

McMartin, I., Godbout, P.-M., Campbell, J.E., Tremblay, T., and Behnia, P., 2021. A new map of glacigenic features and glacial landsystems in central mainland Nunavut, Canada; Boreas, v. 50, no. 1, p. 51–75. https://doi.org/10.1111/bor.12479

Miller, G.H., 1980. Late Foxe glaciation of southern Baffin Island, N.W.T., Canada; Geological Society of America Bulletin, v. 91, no. 7, p. 399–405. https://doi.org/10.1130/0016-7606(1980)91%3c399:LFGOSB%3e2.0.CO%3b2

Natural Resources Canada, 2016. Canadian digital elevation model, 1945–2011; Natural Resources Canada. <https://open.canada.ca/data/en/dataset/7f245e4d-76c2-4caa-951a-45d1d2051333> [accessed July 2021]

Netterville, J.A., Dyke, A.S., Thomas, R.D., and Drabinsky, K.A., 1976. Terrain inventory and Quaternary geology, Somerset, Prince of Wales and adjacent islands; in Report of activities, part A; Geological Survey of Canada, Paper 76-1A, p. 145–154. https://doi.org/10.4095/104183

North Arrow Minerals Inc., 2018. Mel project, NU, samples results with kimberlite; North Arrow Minerals corporate update for May 2018. <http://www.northarrowminerals.com/_resources/Mel%20Project_Probed-Normed%20Samples_with%20Kimberlite_v6.png> [accessed August 2019]

Ocean Mapping Group, 2019. Multibeam bathymetric data; Ocean Mapping Group, University of New Brunswick. <http://www.omg.unb.ca/arctic-mapping/> [accessed August 2020]

Ozyer, C., 2011. Ice-movement history and kimberlite indicator mineral dispersal study, Pelly Bay, lower Boothia Peninsula, and Wager Plateau areas, Nunavut, Canada; Ph.D. thesis, Paper 226, University of Western Ontario, London, Ontario, 187 p.

Ozyer, C.A. and Hicock, S.R., 2006. Ice-movement history, drift prospecting, and marine incursion in the Darby Lake and Arrowsmith River map areas, southern Boothia Peninsula, Nunavut; Geological Survey of Canada, Current Research 2006-C1, 9 p. https://doi.org/10.4095/221946

Pendleton, S., Miller, G., Lifton, N., and Young, N., 2019. Cryosphere response resolves conflicting evidence for the timing of peak Holocene warmth on Baffin Island, Arctic Canada; Quaternary Science Reviews, v. 216, p. 107–115. https://doi.org/10.1016/j.quascirev.2019.05.015

Porter, C., Morin, P., Howat, I., Noh, M.-J., Bates, B., Peterman, K., Keesey, S., Schlenk, M., Gardiner, J., Tomko, K., Willis, M., Kelleher, C., Cloutier, M., Husby, E., Foga, S., Nakamura, H., Platson, M., Wethington, M.J., Jr., Williamson, C., Bauer, G., …and Bojesen, M., 2018. ArcticDEM, version 1; Harvard Dataverse. https://doi.org/10.7910/DVN/OHHUKH

Prest, V.K., Grant, D.R., and Rampton, V.N., 1968. Glacial map of Canada; Geological Survey of Canada, Map 1253A, scale 1:5 000 000. https://doi.org/10.4095/108979

Shaw, J., Potter, D.P., and Wu, Y., 2019. Geomorphic diversity and complexity of the inner shelf, Canadian Arctic Archipelago, based on LiDAR and multibeam sonar surveys; Canadian Journal of Earth Sciences, v. 57, no. 1, p. 123–132. https://doi.org/10.1139/cjes-2018-0312

Sim, V.W., 1962. The physiography of Melville Peninsula; Ph.D. thesis, McGill University, Montréal, Quebec, 326 p.

Simon, Q., St-Onge, G., and Hillaire-Marcel, C., 2012. Late Quaternary chronostratigraphic framework of deep Baffin Bay glaciomarine sediments from high-resolution paleomagnetic data; Geochemistry, Geophysics, Geosystems, v. 13, no. 11, art. Q0AO03, 24 p. https://doi.org/10.1029/2012GC004272

Simon, Q., Hillaire-Marcel, C., St-Onge, G., and Andrews, J.T., 2014. North-eastern Laurentide, western Greenland and southern Innuitian ice stream dynamics during the last glacial cycle; Journal of Quaternary Science, v. 29, no. 1, p. 14–26. https://doi.org/10.1002/jqs.2648

Simon, K.M., James, T.S., Henton, J.A., and Dyke, A.S., 2016a. A glacial isostatic adjustment model for the central and northern Laurentide Ice Sheet based on relative sea level and GPS measurements; Geophysical Journal International, v. 205, no. 3, p. 1618–1636. https://doi.org/10.1093/gji/ggw103

Simon, Q., Thouveny, N., Bourlès, D.L., Nuttin, L., Hillaire-Marcel, C., and St-Onge, G., 2016b. Authigenic ^{10}Be/^{9}Be ratios and ^{10}Be-fluxes (^{230}Th$_{xs}$-normalized) in central Baffin Bay sediments during the last glacial cycle: paleoenvironmental implications; Quaternary Science Reviews, v. 140, p. 142–162. https://doi.org/10.1016/j.quascirev.2016.03.027

Staiger, J.K.W., 2005. Glacial erosion in Atlantic and Arctic Canada determined by terrestrial in situ cosmogenic nuclides and ice sheet modeling; Ph.D. thesis, Dalhousie University, Halifax, Nova Scotia, 244 p.

Staiger, J.W., Gosse, J., Little, E.C., Utting, D.J., Finkel, R., Johnson, J.V., and Fastook, J., 2006. Glacial erosion and sediment dispersion from detrital cosmogenic nuclide analyses of till; Quaternary Geochronology, v. 1, no. 1, p. 29–42. https://doi.org/10.1016/j.quageo.2006.06.009

Stokes, C.R., Clark, C.D., and Storrar, R., 2009: Major changes in ice stream dynamics during deglaciation of the north-western margin of the Laurentide Ice Sheet; Quaternary Science Reviews, v. 28, no. 7-8, p. 721–738. https://doi.org/10.1016/j.quascirev.2008.07.019

Stokes, C.R., Tarasov, L., and Dyke, A.S., 2012. Dynamics of the North American ice sheet complex during its inception and build-up to the last glacial maximum; Quaternary Science Reviews, v. 50, p. 86–104. https://doi.org/10.1016/j.quascirev.2012.07.009

Stokes, C.R., Margold, M., Clark, C.D., and Tarasov, L., 2016. Ice stream activity scaled to ice sheet volume during Laurentide Ice Sheet deglaciation; Nature, v. 530, no. 7590, p. 322–326. https://doi.org/10.1038/nature16947

Sugden, D.E., 1978. Glacial erosion by the Laurentide Ice Sheet; Journal of Glaciology, v. 20, no. 83, p. 367–391. https://doi.org/10.1017/S0022143000013915

Sugden, D.E. and Watts, S.H., 1977. Tors, felsenmeer, and glaciation in northern Cumberland Peninsula, Baffin Island; Canadian Journal of Earth Sciences, v. 14, no. 12, p. 2817–2823. https://doi.org/10.1139/e77-248

Taylor, R.S., 1956. Glacial geology of north-central Keewatin, Northwest Territories, Canada; Bulletin of the Geological Society of America, v. 67, no. 8, p. 943–956. https://doi.org/10.1130/0016-7606(1956)67[943:GGONKN]2.0.CO%3b2

Tremblay, T., 2017. Advances in the surficial geology study of Boothia Peninsula, central Nunavut; in Summary of activities 2017; Canada-Nunavut Geoscience Office, p. 21–36.

Tremblay, T., 2018. Cold-based glaciers terrain in the northeastern Canadian Shield; CANQUA/AMQUA 2018 meeting, Ottawa, Ontario, Program with Abstracts, p. 92.

Tremblay, T., 2021. Geochemistry and mineralogy of glacial sediments and geomorphology of the Jungersen River area, northwestern Baffin Island, Nunavut; in Summary of activities 2020; Canada-Nunavut Geoscience Office, p. 47–62.

Tremblay, T. and Godbout, P.M., 2018. Surficial geology of the north coast of Fury and Hecla Strait, northwestern Baffin Island, Nunavut; in Summary of activities 2018; Canada-Nunavut Geoscience Office, p. 107–120.

Tremblay, T. and Gosse, J.C., 2019. Cosmogenic isotopes transect on the northeastern Laurentide ice sheet cold-based plateaus; INQUA 2019, Dublin, Ireland, Abstract book, p. 1697.

Tremblay, T. and Lamothe, M., 2019. A conceptual framework for the spatial and chronological variations in the intensity of glacial flow within the Boothia–Lancaster ice stream; INQUA 2019, Dublin, Ireland, Abstract book, p. 2837.

Tremblay, T. and Paulen, R., 2012. Glacial geomorphology and till geochemistry of central Melville Peninsula, Nunavut; Geological Survey of Canada, Open File 7115, 46 p. https://doi.org/10.4095/290993

Tremblay, T., Ryan, J.J., and James, D.T., 2007. Ice-flow studies in Boothia mainland (NTS 57A and 57B), Kitikmeot region, Nunavut; Geological Survey of Canada, Open File 5554, 16 p. https://doi.org/10.4095/224165

Tremblay, T., Ryan, J.J., James, D.T., and Kjarsgaard, I.M., 2009. Kimberlite indicator mineral survey and ice flow studies in Boothia mainland (NTS 57A, 57B, 57C and 57D), Kitikmeot region, Nunavut; Geological Survey of Canada, Open File 6040, 31 p. https://doi.org/10.4095/248154

Tremblay, T., Day, S., Shirley, J., Smith, K.A., and McNeil, R., 2016a. Geochemical, mineralogical and sedimentological results from till, stream and lake sediment and water samples in the Sylvia Grinnell Lake area, Baffin Island, Nunavut; in Summary of activities 2016; Canada-Nunavut Geoscience Office, p. 13–26.

Tremblay, T., Lamothe, M., and Paulen, M.C., 2016b. Glacial geomorphology and till geochemistry and mineralogy of southern Melville Peninsula, Nunavut; Geological Survey of Canada, Open File 7494, 50 p. https://doi.org/10.4095/299550

Tremblay, T., Forget Brisson, L., Hardy, F., Lamothe, M., and Gosse, J.C., 2020a. Chronostratigraphy of pre-LGM sediments on Bylot Island, Nunavut; GSA 2020 Connects Online; Geological Society of America, Abstracts with Programs, v. 52, no. 6, p. 2020. https://doi.org/10.1130/abs/2020AM-359908

Tremblay, T., Sasseville, C., and Godbout, P.M., 2020b. Geochemistry and mineralogy of glacial sediments in the Fury and Hecla area, northwestern Baffin Island, Nunavut; in Summary of activities 2019; Canada-Nunavut Geoscience Office, p. 51–64.

Utting, D.J., Little, E.C., Young, M.D., McCurdy, M.W., Dyke, A.S., and Girard, I., 2008. Till, stream-sediment and bedrock analyses, north Baffin Island, Nunavut (NTS 37E, F, G, H and 47E); Geological Survey of Canada, Open File 5742, 14 p. https://doi.org/10.4095/225113

Veillette, J.J., Dyke, A.S., and Roy, M., 1999. Ice-flow evolution of the Labrador sector of the Laurentide Ice Sheet: a review, with new evidence from northern Quebec; Quaternary Science Reviews, v. 18, no. 8-9, p. 993–1019. https://doi.org/10.1016/S0277-3791(98)00076-6

Wheeler, J.O., Hoffman, P.F., Card, K.D., Davidson, A., Sanford, B.V., Okulitch, A.V. and Roest, W.R., 1996. Geological map of Canada / Carte géologique du Canada; Geological Survey of Canada, Map 1860A, scale 1:5 000 000. https://doi.org/10.4095/208175